Politecnico di Torino

Politecnico di Torino

Master of science in Energetic and Nuclear Engineering
Academic year 2021/2022
Graduation session July 2022

ARC reactor: neutronic and activation analysis of high-entropy alloys for the vacuum vessel

Advisors:
Prof. Massimo Zucchetti
Prof. Raffaella Testoni
Co-Advisors:
Dr. Samuele Meschini
Dr. Stefano Segantin

Candidate:
Davide Pettinari

Alla mia famiglia

Abstract

We live in a time when we need to increase energy production and reduce CO_2 emissions. In this perspective, nuclear energy is characterised by one of the lowest emissions values per unit of energy produced and at the same time it may provide energy in a constant and controllable way. The objective of this thesis is the modelling of the vacuum vessel for Affordable Robust Compact (ARC) fusion reactor: an approximately 190 MWe tokamak reactor of small size in order to reduce the cost and the complexity of such a facility. ARC is under development by the Massachusetts Institute of Technology (MIT) and PSFC (Plasma Science and Fusion Centre). The schematisation of its geometry was made gradually, starting from a very simplified geometry to a D shape model, to best approximate reality.

Tritium breeding ratio, neutron flux, neutron spectra and neutron currents were computed by OpenMC.

The study firstly analysed the single blanket module geometry with a first wall of tungsten, Inconel 718 as the structural material, FLiBe as breeding blanket and coolant, and beryllium as neutron multiplier. An additional layer made of Tungsten carbide was inserted as a shield and reflector to increase the TBR. To optimise the TBR we replaced the structural material with a high-entropy alloy and perform a sensitivity study on it to obtain the best composition.

An assessment of the 184W tailoring technique to study the influence on the TBR was made on the alloys. Through the use of high-entropy alloys, it was possible to remove the beryllium layer, as it is expensive, toxic and contains traces of uranium. The plasma source needed to be modified to best represent the real case. Starting with a homogeneous, isotropic source with a simple box geometry, the simulations were carried out with a tokamak plasma source from the 'OpenMC-plasma-source' package.

Finally, the FISPACT-II program studied the neutron induced activation of materials throughout the vacuum vessel and the effect that impurities can have on these materials.

Materials activation is expected to affect the reactor economy in terms of decommissioning and management of radioactive waste as well as affecting public acceptance of this energy source, as activated materials could be associated with the problem of long-life waste typical of fission reactors. In this regard, the activation analysis showed the superiority of high-entropy alloys, since they allow a faster decay after being irradiated than Inconel-718.

I want to thank my supervisors Massimo Zucchetti, Raffaella Testoni, Samuele Meschini and Stefano Segantin for the important opportunity they gave me.
A special thanks goes to my family, because without them all this would have never been possible, to my friends and to all the people with whom I shared this amazing journey.
Finally, a last but huge thanks goes to all the teachers I had, for giving me the enthusiasm and passion for these subjects.

Contents

List of Figures

List of Tables

Chapter 1

1 Introduction to nuclear fusion energy

The policies and measures implemented to reduce greenhouse gas emissions have enabled compliance with the 2020 emission targets. However, further efforts are needed to achieve the future targets, given the new target (set by the European Climate Act) of a net internal reduction of greenhouse gas emissions of at least 55% by 2033 and the target of "climate neutrality" by 2050 [1].

Nuclear fusion will play a key role in achieving this objective. The main advantage of nuclear fusion is the production of electricity without the release into the atmosphere of pollutants such as nitrogen oxides or sulphur oxides or carbon dioxide, the main greenhouse gas.

Further advantages of this technology are linked to the fact that there are no chain reactions, no negative reaction products (alpha particle and neutron), there is no spontaneous divergence of the power produced by the plant, there is no open fuel cycle. In addition, the fusion reaction of deuterium and tritium nuclei for heat generation is intrinsically safe because a variation from the optimum gas density value, the temperature or the magnetic confinement effectiveness is sufficient to turn off the reaction.

Fusion is a nuclear reaction; therefore, it makes some components radioactive. Materials subjected to a large flow of high-energy neutrons acquire a degree of radioactivity such as to be considered "medium/low level waste" which must be properly treated. For the future fusion reactor, the use of low-activation metal alloys is envisaged. Consequently, all these materials fall below the threshold of radiological relevance after a time not exceeding 100 years from the discharge from the reactor. For this reason, consideration has been given to the possibility of conditioning and disposal on the same site as the plant, without the need to transfer them to a permanent surface storage.

The following thesis was carried out in collaboration with the Massachusetts Institute of Technology (MIT) on the affordable, robust, compact (ARC) reactor.

This reactor has the peculiarity of having small dimensions that result in low construction costs. Moreover, thanks to the studies that have been done on this reactor, new important technologies are applied, such as molten salts for the breeding blanket and superconducting magnets at high temperature [2].

The many studies conducted on structural materials [3] [4] have motivated the study of this thesis, in order to look for a high entropy alloy suitable to replace the structural material that was intended to use. The aim was to ensure low activation of the vacuum vessel, a higher TBR due to the presence of neutron multipliers in the alloy and lower plant costs by removing the beryllium layer.

This first section is an introduction to the physics of nuclear fusion, to how to achieve it on Earth, to the most promising reactions, to the ARC reactor and to the new structural materials to be used. The second chapter focuses on a neutron analysis of this proposed new alloy.

In the third, an activation analysis is carried out.

1.1 Fusion reaction

The fusion reaction is most commonly known as the energy source that powers the stars. An example of a ration within the Sun is between four protons that fuse and form a helium nucleus, two positrons and two neutrinos.

As for the earth, the most feasible fusion reaction is that between a nucleus of deuterium (a neutron, a proton) and a nucleus of tritium (two neutrons, a proton), which is a reaction of only nuclei. The two nuclei merge leading to the stable configuration formed by a helium nucleus and an isolated neutron.

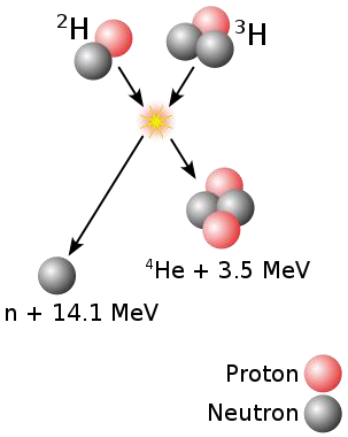

Fig. 1.1: *Fusion of deuterium with tritium creating helium-4, freeing a neutron, and releasing 17.59 MeV as kinetic energy of the products [5].*

The potential of this reaction is to be unlimited and to be almost clean. From the fuel point of view, this reaction consists of:

- Deuterium: it is obtained from sea water, so it is an unlimited element
- Tritium: is a radioactive isotope with a half-life of about 12 years, it can be produced from lithium.

Reaction products are produced with a certain energy which serves different purposes:

- The energy with which the α particle is produced is useful to keep the mixture of deuterium and tritium warm, because if it is not hot enough the fusion reaction does not take place
- The energy with which the neutron is produced is the real source of usable energy. The neutron slows down, from the microscopic point of view, it yields its kinetic energy by converting it into heat inside a solid medium that will warm up.

When the neutron is in the solid means it can slow down through collisions heating the means, or it can be captured by a nucleus. In the latter case the neutron can activate the nucleus, this occurs when the nucleus becomes unstable after neutron absorption. After a certain period of time, it can take place a transmutation that leads to the emission of a gamma ray. This phenomenon can lead to the activation of structures that originally were not.

The reaction mentioned above is not the only fusion reaction achievable.

The most important reactions for fusion are [6]:

D-D: $$ {}_1^2H + {}_1^2H \rightarrow \begin{cases} {}_1^3H + {}_1^1H + 4.03\ MeV \\ {}_2^3He + {}_0^1n + 3.27\ MeV \end{cases} \quad (1.1) $$

D-T: $$ {}_1^2H + {}_1^3H \rightarrow {}_2^4He + {}_0^1n + 17.59\ MeV \quad (1.2) $$

D-^{3}He: $$ {}_1^2H + {}_2^3He \rightarrow {}_2^4He + {}_1^1H + 18.35\ MeV \quad (1.3) $$

The reactions mentioned above are the best candidates to support a fusion reaction. From the graph shown in figure 1.2 it is deduced that the energy of the deuterium is sufficiently smaller than the minimum one, the cross-section results almost null; therefore, the probability to make such reactions happen is almost zero. Thus, the D-T reaction is the most promising as it has the minimum energy to be provided lower than the other reactions.

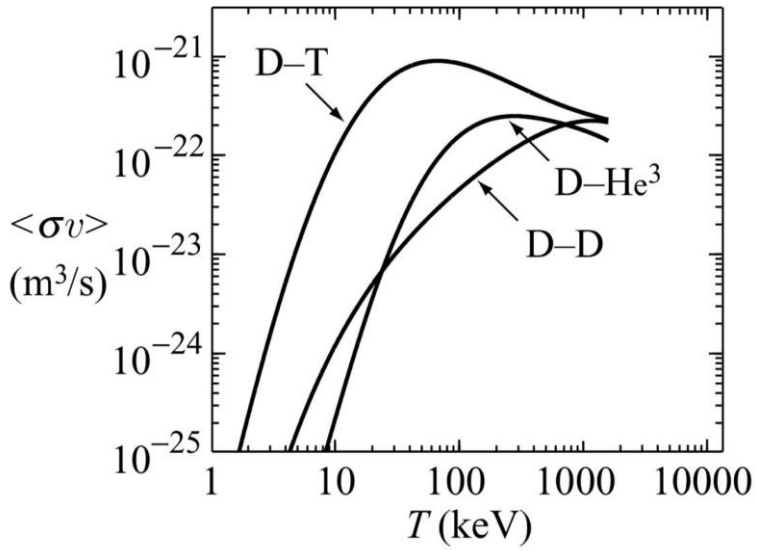

Fig. 1.2: *The fusion reaction rate increases rapidly with temperature until it maximizes and then gradually drops off. The DT rate peaks at a lower temperature (about 70 keV, or 800 million kelvin) and at a higher value than other reactions commonly considered for fusion energy [7].*

The other reactions are interesting because:

- D-D reaction: there is no tritium between the reagents; therefore, there is no radioactive material and only sea water can produce the fuel. The problem with this reaction is that it can produce tritium and one neutron (activation problem)
- D-^{3}He reaction: neither tritium nor neutrons are produced, the problem in this reaction is that deuterium has the same probability of reacting with helium-3 but also with other deuterium. A further problem is the minimum energy to be provided, much larger than in the D-T reaction. Moreover, ^{3}He is not found on earth, except that from tritium decay.

In order to obtain controlled thermonuclear fusion, a certain amount of kinetic energy is required, and it can be supplied in the form of thermal energy. The difficulty lies in the fact that, in order for the D-T reaction to take place, the reagents must be brought to energies corresponding to temperatures of the order of 100 million degrees. The state of matter at such temperatures is defined as plasma (fully ionised gas).

1.2 Fusion reactor

Fusion reactor is a device that permits the controlled release of fusion energy.

Plasma consists of charged particles (deuterium and tritium ions) and can be confined by a magnetic field. Different configurations have been studied in order to obtain such confinement, namely the reversed field pinch (RFP), the stellarator that generates the magnetic field using only magnets and the Tokamak which is the configuration that has given better results [8].

The magnetic field in the Tokamak is generated by a set of magnets, each of which has its own particular function:

- Inner poloidal field coils: by circulating a pulsed current, the solenoid generates a time-varying magnetic field that induces a variable current in the plasma that leads to the formation of a poloidal magnetic field (necessary to avoid drift of plasma particles towards the vessel walls)
- Toroidal field coils: they form a toroidal magnetic field forcing charged plasma particles to flow along that direction
- Outer poloidal field coils: they permit to control the position of the plasma by generating vertical fields.

The union of the generated magnetic fields produces a resultant magnetic field consisting of helical field lines.

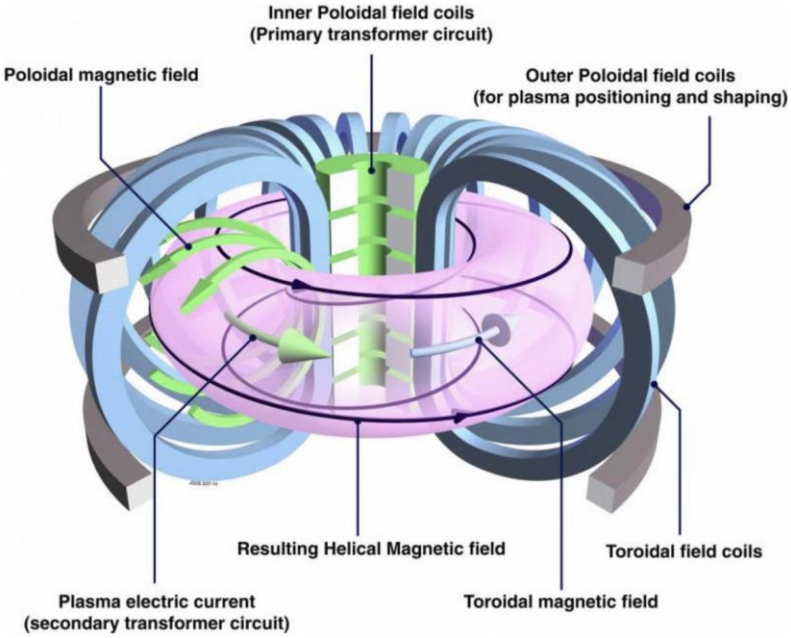

Fig. 1.3: *Schematic of a Tokamak chamber and magnetic profile [9].*

In addition to magnets, the main components of a Tokamak are the vacuum vessel, the divertor and the cryostat.

The vacuum vessel comprises the blanket and the first wall which is the first material that interfaces to plasma and is usually made of tungsten, since it offers maximum wall strength and is difficult to erosion.

Each of these components has a specific function, in particular the blanket has the task of extracting the power deposited by neutrons, extracting and cultivating tritium (it needs a

Breeder and a multiplier) and finally together with the vacuum vessel it has the shielding function to preserve the magnets and external components of the reactor.

There are two very important values needed to be met to build a fusion reactor:

- the ratio between the power produced in the vacuum chamber and the power absorbed in the blanket has to be greater than one;
- the tritium breeding ratio TBR, defined as the ratio of tritium produced in the blanket divided by tritium burned in the plasma, must be greater than 1 to allow for self-sufficiency.

It is necessary to ensure that the reaction takes place and, at the same time, produce an extra amount to store, which can be used to turn on the reactor once it is stopped for maintenance or to turn on new reactors. Tritium can be obtained in this way or as a radioactive product from fission reactors, but only that of fission reactors is not sufficient to ignite new reactors.

Tritium can be generated by neutron absorption in lithium, according to the two reactions [6]:

$$^{6}_{3}Li + {}^{1}_{0}n \rightarrow {}^{3}_{1}H + {}^{4}_{2}He + 4.8\ MeV \quad (1.4)$$

$$^{7}_{3}Li + {}^{1}_{0}n \rightarrow {}^{3}_{1}H + {}^{4}_{2}He + {}^{1}_{0}n - 2.5\ MeV \quad (1.5)$$

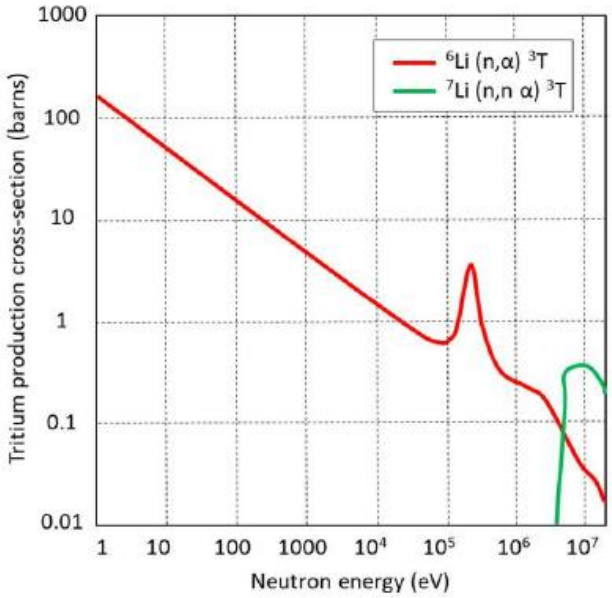

Fig. 1.4: *Tritium production cross section up to 14 MeV for ⁶Li and ⁷Li [10].*

Natural mixture of lithium contains 7.5% of 6Li and the other 92.5% of 7Li. The two reactions have very different features: while the first one is exothermic, the second one is endothermic (it is a threshold reaction, a minimum energy is required for it to happen). In the figure 4 the

cross-sections corresponding to the two reactions are shown: while 6Li reaction has a very high cross-section (especially in the low-energy region), the 7Li reaction works with the high-energy neutrons and has a threshold. 7Li produces an additional neutron that is available for a successive reaction, which means that TBR greater than 1 is possible (for one tritium burnt in the plasma, it is possible to produce more than one tritium in the blanket).

Actually, it is not so easy to reach a TBR greater than 1, since there are divertor and heating devices that do not produce tritium and can take place parasitic neutronic capture and neutron leakages

This means that in order to obtain a TBR greater than 1, a neutron multiplier layer is inserted in the design, which attracts the reaction (n, 2n), increases the number of neutrons and, consequently, increases the production of tritium in the blanket.

1.3 ARC: Affordable, Robust and Compact reactor

In 2021, there was a historic breakthrough in controlled thermonuclear fusion: the realisation of a high temperature superconducting magnet based on rare earth barium copper oxide (REBCO superconductors) designed and built by the Commonwealth Fusion Systems (CFS) and scientists of the Plasma Science and Fusion Center (PFSC) [11].

Thanks to this it is possible to build the ARC reactor, a conceptual tokamak design, designed by MIT to produce energy by 2033.

Superconductive magnets are composed by substances that can enter the so-called "Meissner state" [12], a condition in which the material generates a strong magnetic field outside of it but essentially no magnetic field within it. This condition is maintained only if it is sufficiently low temperature and breaks down also if the field is too strong. High temperature superconductors (HTS) materials, for the design of tokamak toroidal field (TF) magnets, offer several attractive advantages with respect to low temperature superconductors (LTS):

- Larger temperature margin (current technologies involved the use of supercritical helium at a temperature of 4.5 K in order to make superconductive magnets, now with REBCO tapes is sufficient to stay below 80 K);
- Possibility to operate at higher magnetic fields and temperature.

As the acronym itself suggests, this reactor (based on the deuterium-tritium reaction) has the characteristic of being small despite a fusion power of 520 MW. Its major radius measures only 3.3 m and its minor radius 1.13 m which are much smaller than the size of the other reactors

under study in the world. The small size of this reactor permits low construction costs, which is one of the goals of the project.

This reactor is designed to produce 190 MWe, about three times the energy spent to operate and maintain the fusion reaction.

The use of REBCO tapes makes the maintenance of the plant much easier. Actually, these materials can be spliced, so it is possible to divide the TF coil in half and remove the entire vacuum vessel to replace it [13].

The reactor design, the inboard radial build and the most important design parameters are shown in the figures 1.5, 1.6 and in table 1.

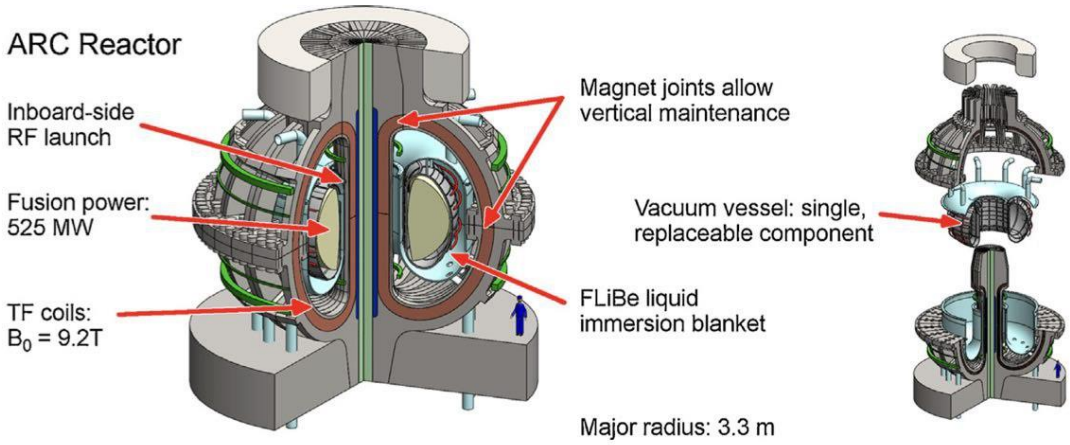

Fig. 1.5: *The ARC reactor with a picture of the single piece vacuum vessel (on the right) [2].*

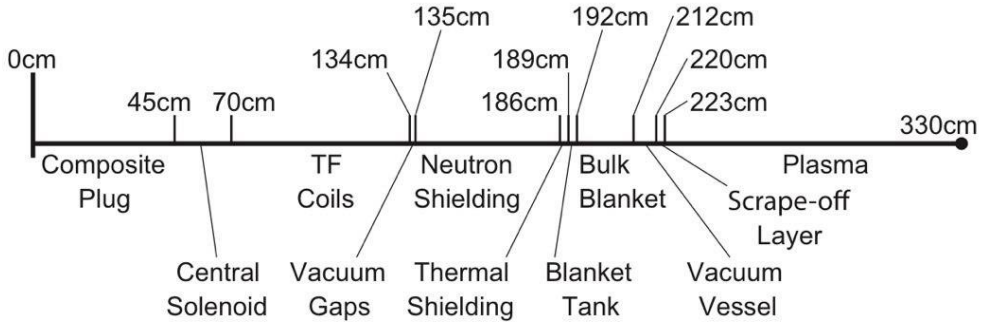

Fig. 1.6: *The ARC reactor inboard radial build [2].*

Table 1-1 *List of significant ARC design parameters [2].*

Design parameter	Value
Fusion power	525 MW
Total thermal power	708 MW
Planta thermal efficiency	0.40
Total electric power	283 MW
Net electric power	190 MW
Power multiplication factor	3.0
Major radius	3.3 m
Plasma semi-minor radius	1.13 m
Plasma elongation	1.84
Plasma volume	141 m^3
Toroidal magnetic field	9.2 T
Peak on-coil magnetic field	23 T
Plasma current	7.8 MA
Tritium breeding ratio	1.1
Avg. temperature	14 keV
On-axis temperature	27 keV
Energy confinement time	0.64 s

1.3.1 Choice of breeder

In the breeding blanket there are at least 4 different functional materials: tritium breeder, neutron multiplier, tritium carrier (to take tritium out of the blanket) and coolant. The breeder can be solid or liquid. Liquid breeders can be used also as coolant, and they can be liquid metal or molten salt.

The ARC reactor uses a liquid blanket of FLiBe, a molten salt composed of lithium fluoride and beryllium fluoride. It ensures a TBR greater than 1.1, because it contains lithium and beryllium serving respectively as a tritium Breeder and a neutron multiplier.

The use of a molten salt involves pros and cons:

- Pros: no reactivity with air or water, limited MHD (Magneto hydro dynamics) issues, because it does not contain metals.
- Cons: high melting point (459°C), high Prandtl number (which entails a low thermal conductivity), they have a complex chemistry, and they are very corrosive.

ARC is designed in such a way that the FLiBe flows through a channel located inside the vacuum vessel poloidally and the vacuum vessel itself is surrounded by a FLiBe pool. This design was chosen to optimise the TBR, increase the shielding function and remove the heat.
Actually, the FliBe will go into a heat exchanger to power a high efficiency helium Brayton cycle that will produce electricity.
Approximately 26% of the tritium produced within the reactor is generated in the FLiBe cooling channel within the vacuum vessel wall. In this location, there is a higher flux of fast neutrons relative to outside the VV due to the coolant channel's proximity to the core plasma [14].

1.3.2 Choice of structural materials

In ARC, Inconel-718 has been chosen as the material to realise the vacuum vessel, because it has an excellent corrosion resistance placed in contact with the FLiBe [15], and the ability to maintain high strength and corrosion resistance when it is placed at high temperatures.
Corrosion resistance to this alloy is provided by the presence of nickel which at the same time causes activation-related problems, especially during disposal.
However, further research has been carried out and it has been shown that replacing this alloy with Eurofer97 or vanadium alloys allows higher TBR values [16]. This is largely due to the fact that the vanadium alloy and Eurofer97 have a lower density than Inconel718, a lower absorption cross section and they act as neutron multipliers.
These proposed alloys have shown better results in activation studies proving to be low activation material. Actually, dose rate decays to low enough values such as to permit hands-on operation within a relatively short decay time, and the material recycling outside the nuclear industry within a feasible intermediate storage.
In addition, multicomponent alloys defined as HEAs (high entropy alloys, so called because of the high entropy of mixing) have also been proposed.

1.4 High-entropy alloys

High entropy alloys consist of at least 5 elements and their peculiarity is that they are present in more or less equal quantities.
This feature allows to obtain properties that are not normally obtainable with traditional alloys and to obtain a mix of properties that generally conflict with each other such as strength and ductility. In addition, even at high temperature the behaviour of these alloys, if properly designed, is superior to traditional materials.

These alloys aim to overcome the limitations of current materials because nowadays there is the necessity to reduce emissions and to have systems increasingly efficient in terms of energy. Consequently, having materials that work properly in extreme conditions brings a very important advantage.

In particular, high entropy alloys have [17]:

- Excellent specific resistance (can withstand high loads before failure occurs)
- Superior mechanical performance at elevated temperatures
- Exceptional ductility qualities
- Toughness at cryogenic temperatures
- Superparamagnetism (form of magnetism which appears in small ferromagnetic or ferrimagnetic nanoparticles) and superconductivity (electrical resistance vanisches and magnetic flux fields are ejected from the material)

The high entropy mixing of these alloys at high temperatures facilitates the formation of single-phase solid solutions. Therefore, thanks to the slow diffusion of the constituent elements, excellent mechanical performance occurs at high temperatures

In this thesis, an alloy of vanadium, chromium, tungsten, tantalum and titanium is proposed to replace Inconel-718 as a structural material for the vacuum vessel.these elements were chosen because if they are irradiated by a neutron flux, they can allow for neutron multiplication and thus lead to an increase in TBR, while at the same time presenting low activation.

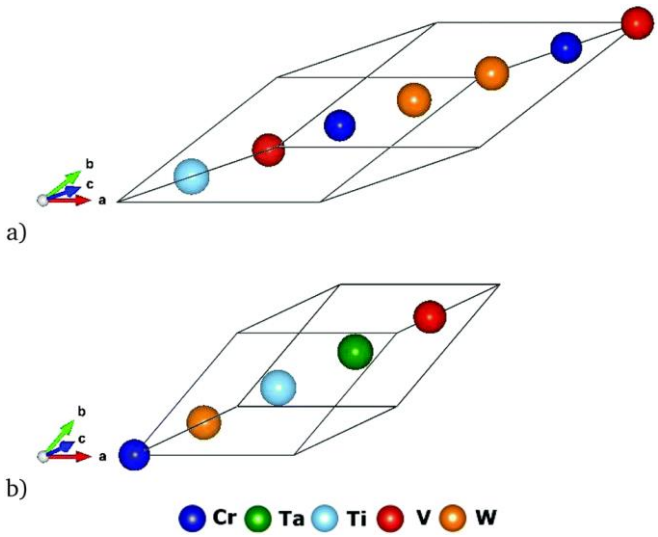

Fig. 1.7: *Quaternary and quinary structures with the lowest enthalpies of mixing: (a) Cr2TiV2W2 and (b) CrTaTiVW [18].*

Chapter 2

2 Neutronic analysis

In this chapter, the Vacuum Vessel is first analysed in a simplified way assuming a cylindrical geometry and a box source in which two types of structural materials are tested.
Then it is tried to model a geometry and a source more similar to reality and to conduct a sensitivity analysis on the high entropy alloy to understand which composition optimises the best production of tritium.
Finally, an isotopic tailoring is conducted on the most promising compositions.

2.1 OpenMC

OpenMC is a community-developed Monte Carlo neutron and photon transport simulation code It was originally developed by members of the Computational Reactor Physics Group at the Massachusetts Institute of Technology [19]. Nowadays several universities, laboratories and organisations contribute to its development.
A basic model consists of:

- A description of the geometry – the problem has to be divided into regions of homogeneous material composition;
- A description of the nuclides in each one material and at what density;
- Parameters telling the code how many particles to simulate and what options to use;
- A list of the physical quantities the code should return at the end of the simulation: questions are needed to get answers, otherwise in a Monte Carlo simulation it would be possible to get only defaults quantities.

2.2 Simplified model

In order to study the neutronic analysis in ARC, it is not necessary to model the entire Vacuum Vessel, but it is sufficient to model a single blanket module. The results obtained for it are then extended to the entire reactor.

It is decided to implement as simple as possible the model using a cylindrical geometry and neglecting the toroidal curvature for two reasons. The first is that it needed fast building and fast running performances. The second is that if tritium production is to be evaluated, for a preliminary study a simple geometry approximates the real case quite well.

So, the main differences between this model and the real geometry are related to the cylindrical shape instead of the D-shape and the toroidal symmetry of the vacuum vessel. The D-shape should not strongly affect the TBR.

The VV configuration is characterised by: 0.1 cm of tungsten as first wall; 1cm of structural materials; 2 cm of flowing FliBe as blanket and coolant; 1 cm of beryllium as neutron multiplier; 3 cm of structural material and roughly 1 m of bulk FliBe in a tank [16].

The inner radius of the cylinder is set to 139.9 cm and the height has been set to 100 cm.

It was chosen to use this value for the inner radius because it allows the plasma volume to be contained and it represents the same first wall surface of the reactor.

No vacuum was left inside as it would have created problems with the neutron simulation, so extremely rarefied hydrogen was placed inside.

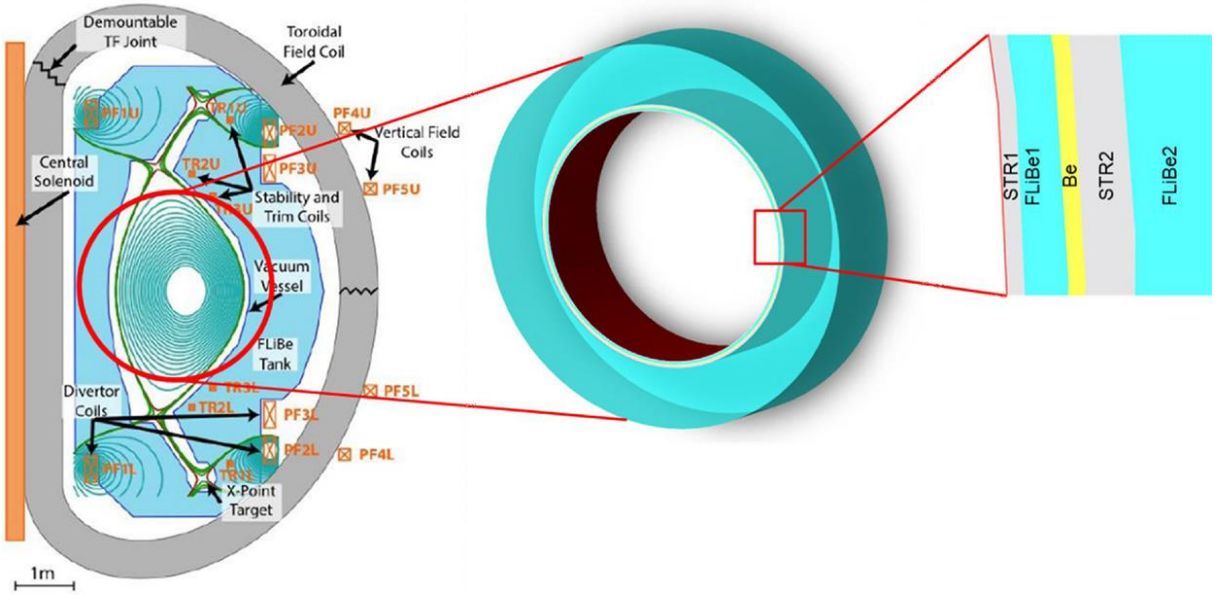

Fig. 2.1: *Original model (left) [14], simplified model (centre) and zoom in of the original configuration, namely tungsten first wall (red), structural layers (STR1, STR2), beryllium as neutron multiplier (Be) and FLiBe's volumes(FLiBe1, FLiBe2 [16].*

The source has been modelled as a homogeneous source box in the cylinder's central axis with height, width and depth set to 100 cm and emitting 14.1 MeV neutrons isotropic.
Using OpenMC neutron transport code the materials for the problem are defined and the temperature and density are also set.

$$\rho_{mix}^{T} = \sum_{i} X_i \cdot \rho_i^T \tag{2.1}$$

Where ρ is the density, T is the set temperature and X is the molar concentration.
Model temperature has been set to 900 K for all the materials, as reference temperature and the densities entered are:

- Tungsten 19.25 g/cm^3
- Inconel-718 8.19 g/cm^3
- High-entropy alloy 10.73 g/cm^3
- FLiBe 1.94 g/cm^3
- Beryllium 1.85 g/cm^3
- Void ('H') 0.0001 g/cm^3

The two structural materials examined have the composition shown in the following tables.

Table 2-1 *Inconel-718 chemical composition by wt% [20].*

Element composition	Al	C	Co	Cr	Cu	Fe	Mo	Ti	Nb	Ni
Inconel-718	0.52	0.021	0.11	19.06	0.02	18.85	3.04	0.93	5.08	53.0

Table 2-2 *High-entropy alloy chemical composition by wt%.*

Element composition	V	Cr	W	Ta	Ti
HEA	20.0	20.0	20.0	20.0	20.0

Next the geometry of the problem is defined by constructing several concentric cylinders and placing two boundary planes to surround the geometry.
Boundary conditions are placed on the planes and on the outer cylinder:

- Vacuum boundary condition is set on the outer cylinder because by hypothesis the neutrons leaving the domain are considered to be non-re-entrant

- Reflective boundary conditions are set on the planes because this assumes a continuous geometry (neutrons do not leave the domain, they would simply go into another blanket module and consequently neutrons from another module can enter in the domain)

Then a material is associated with each region created.
It is important to define the source and the settings that tell the code how many particles to run.
Finally, before running the code are defined the tallies for:

- Neutron flux distribution
- Neutron spectra on the two regions of structural materials (STR1, STR2)
- Neutron current at the boundary (leakage fraction)
- Tritium production distribution
- TBR (total production)

On the breeding blanket the Li-6 enrichment has been kept to 90%. The fact that there is an abundance of Li-6 compared to Li-7 is due to the fact that Li-6 has a higher (n, t) cross section respect to Li-7. In addition, Li-6 has an endothermic reaction with neutrons and therefore increases heat generation in the blanket and consequently the reactor power output increasing, while the exothermic reaction of Li-7 would decrease the reactor thermal power. Despite this in terms of reactor economics, it would be preferable to have a lower enrichment of Li-6 because its abundance in nature is around 7.6% and therefore the enrichment process is very expensive. The reactions of greatest interest occurring in it are:

$$Li6 + n \rightarrow \alpha + T + 4.8\,MeV \quad (2.2)$$

$$Li7 + n \rightarrow \alpha + T + n - 2.5\,MeV \quad (2.3)$$

$$Be9 + n \rightarrow Be8 + 2n \quad (2.4)$$

$$F19 + n \rightarrow F20 \quad (2.5)$$

The code counts all these reactions, in order to provide the results sought.
The simulation involved 30 batches plus 10 inactive, running 10 000 particles for each batch.

2.2.1 Comparative results of the two materials

The first results obtained from the code concern the neutron flux distribution.

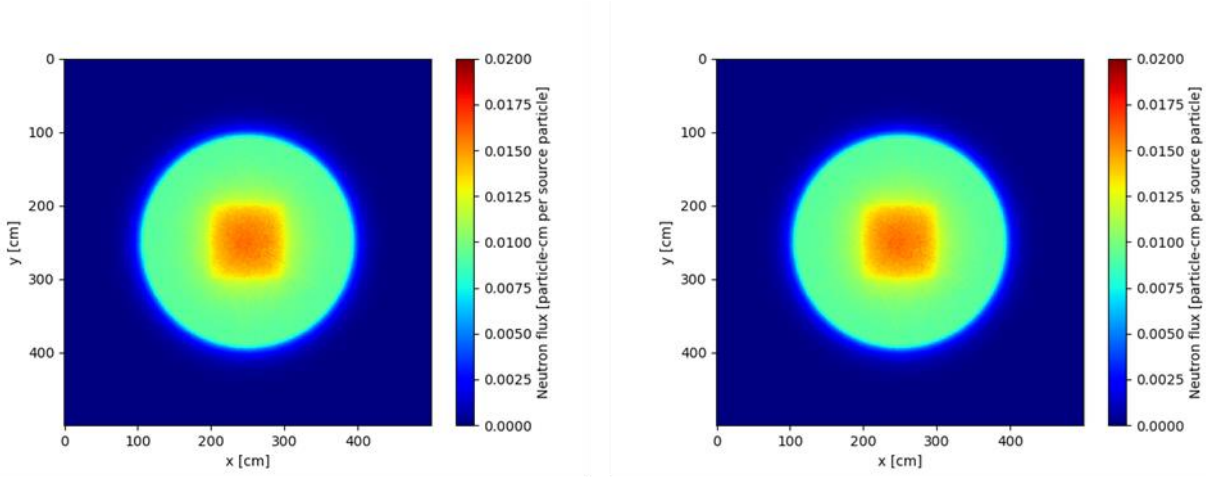

Fig. 2.2: *Neutron flux distribution on VV with Inconel-718 as structural layers (on the left) and High-entropy alloy (on the right).*

What emerges from the comparison of these two trends is that there is no significant difference in the neutron flux by changing structural materials.

Fig. 2.3 and Fig. 2.4 shows the second result that is the neutron spectra in the STR1 and STR2. The neutron spectra show no significant differences across the first layer of structural material, except at low energies (some eV) where the neutron flux through the high-entropy alloy is slightly lower. This is due to the fact that in this alloy there are vanadium and tantalum. These two elements at low energies are characterised by good capture cross sections but in this area almost all incoming neutrons are fast and therefore with high energies because between the plasma (where they are generated at about 14 MeV) and STR1 only one millimetre of first wall is present.

In the neutron spectra through the second layer of structural material, this difference at low energies increases, because some slowed down neutrons can occur due to the collisions in the FLiBe, in the STR1 and in the first wall.

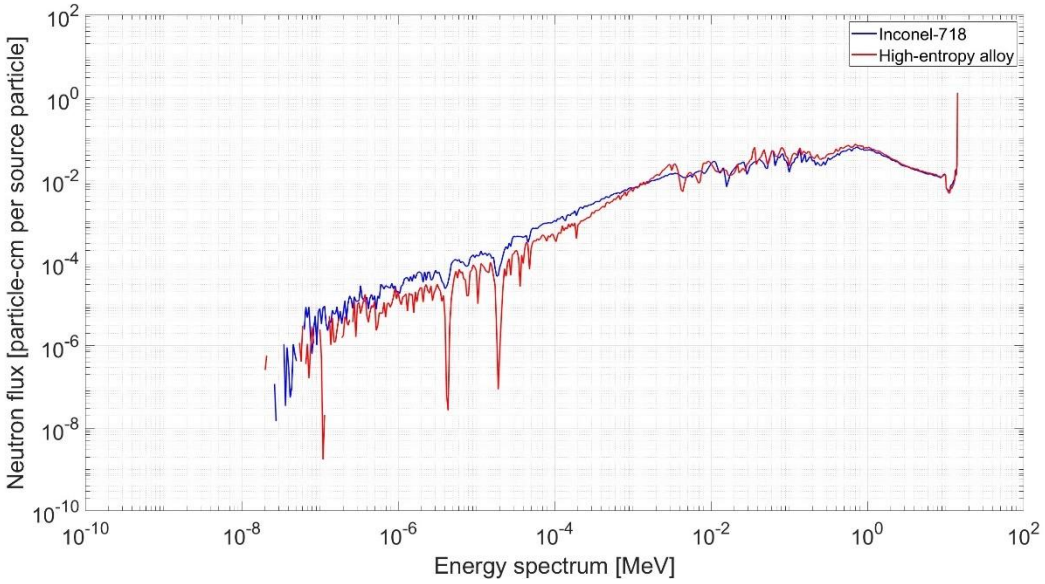

Fig. 2.3: *Neutron spectra in STR1.*

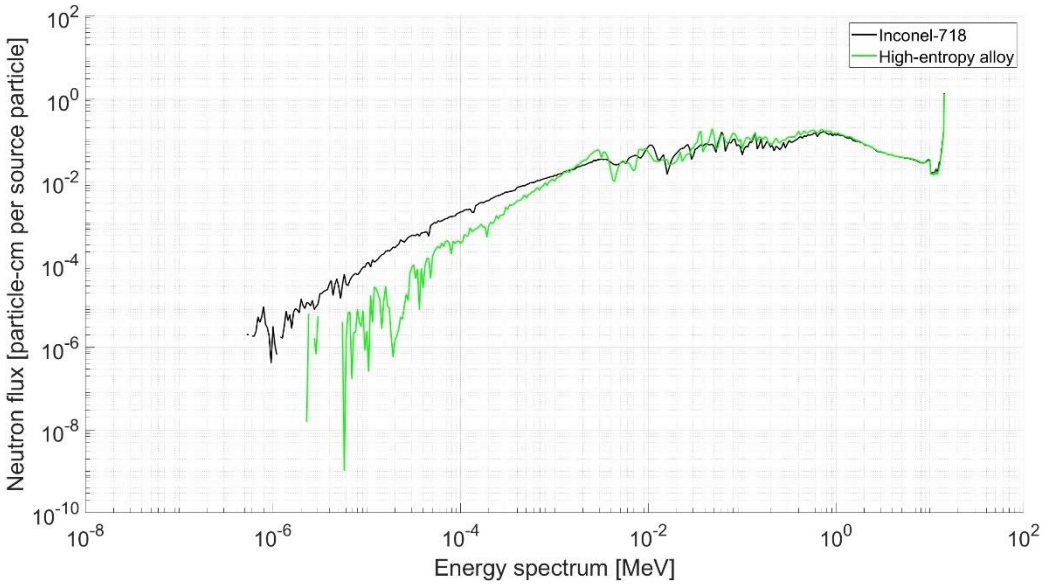

Fig. 2.4: *Neutron spectra in STR2.*

The third result concerns the leakage fraction expressed as particles per source particle. There is no difference; the structure is surrounded by 1 m of bulk FLiBe in a tank which has an excellent shielding function.

Table 2-3 *Neutron current on the external surface [particles per source particle].*

Alloys	Mean value	Standard deviation
Inconel-718	2.94e-04	1.68e-05
HEA	2.78e-04	1.62e-05

Differences can be seen in the production of tritium. Actually, the high-entropy alloy contains tungsten, which acts as a neutron multiplier, so there is a higher TBR in both the inner channel of FLiBE and in the outer tank.

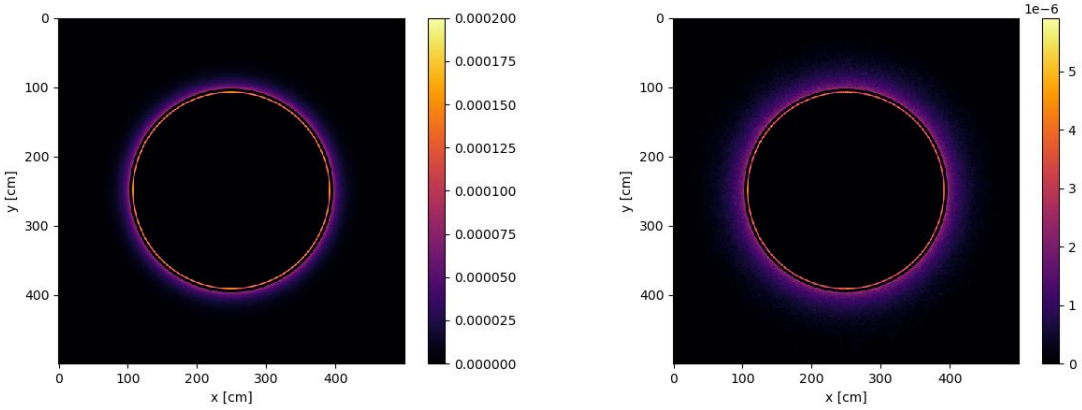

Fig. 2.5: *Tritium generation mesh tally mean result (left) and standard deviation (right) with Inconel-718.*

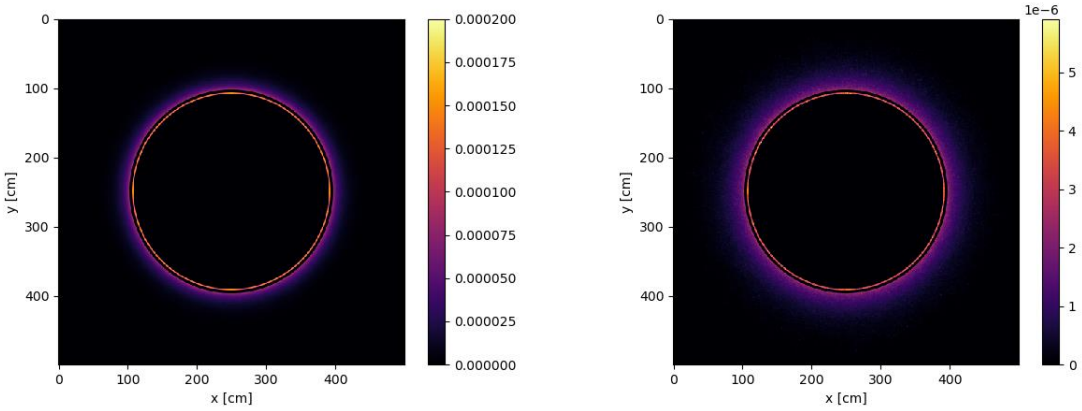

Fig. 2.6: *Tritium generation mesh tally mean result (left) and standard deviation (right) with HEA.*

Table 2-4 *TBR production in FLiBe.*

Alloys	TBR [-]	Standard deviation
Inconel-718	1.072	1.69e-03
HEA	1.14	1.65e-03

2.3 D-shape model

Starting from the previously created geometry, an attempt is made to obtain a D-shape geometry by joining planes and cylinders (Appendix A shows the construction of this model).

The cylinder has an internal radius of 139.9 cm and the height is set to 100 cm, which corresponds to 1/20 of the vessel's length at its major radius [16].

In addition to the shape compared to the previous case, the outer radius of the blanket and the composition of some materials have been changed.

In particular, the outer radius is reduced to 50 cm, as tritium production only occurred in the inner area of the tank; it must be verified that the neutron leakage remains small and acceptable.

In order to improve the TBR, natural tungsten is replaced by W184 in the high entropy alloy and first wall as it is much less absorbent and does not entail a significant increase in reactor economics since it is very abundant in nature.

The high-entropy alloy are not only analysed in the base case as done previously, but 8 different compositions are analysed in order to find the one that best optimises TBR. Since in this configuration beryllium is present both in the molten salt and in the neutron multiplier layer, it is removed and FLiBe is put in its place, thus increasing the inner channel by 1 cm.

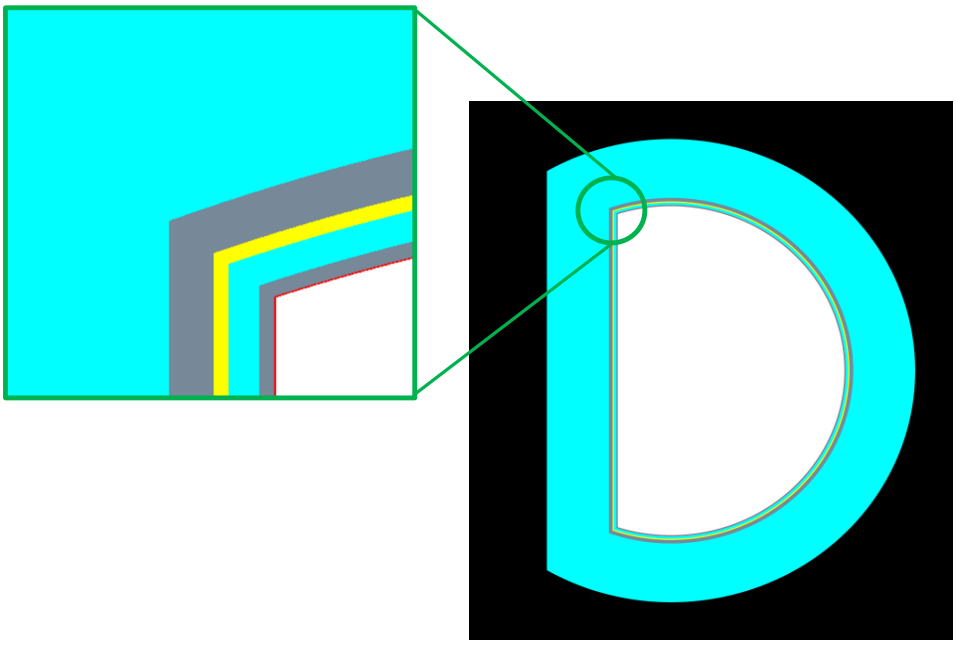

Fig. 2.7: *Geometry of the D-shape model with a zoom of the vessel region (left). Vacuum vessel layers (gray), channel and blanket region (cyan), first wall (red) and neutron multiplier (yellow).*

2.3.1 Tokamak plasma source

In addition to the geometry, the source is also changed to make it as close to reality as possible. Using the 'openmc-plasma-source' package it is possible to create a source with a spatial and temperature distribution of a tokamak plasma. The OpenMC sources are ring sources, which reduces the computational cost and the settings.xml file size.

This package implements the equations that are present in the article [21].

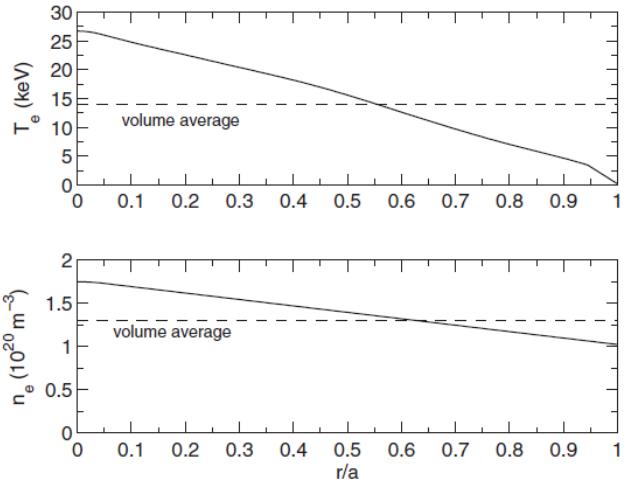

Fig. 2.8: *Radial profiles of electron temperature and electron density in ARC (a is the plasma semi-minor radius and r is the distance from the centre to a) [2].*

Many parameters are needed to apply this model, some of them are extracted in part from Fig.2.8: the pedestal temperature is shown to rise at r/a=0.95, the pedestal density is taken at the same ratio r/a, while the temperature and the density at the separatrix are taken for a ratio r/a=1.

Major and minor radius are inserted in according to the constructed geometry, while the other parameters are provided by the package itself [22].

Fig.2.9 and Fig.2.10 show how the programme constructed the source and the particular density and temperature distributions. Fig.2.11, on the other hand, shows the geometry constructed with the source positioned inside, taking care not to let it collide with the first wall.

An intersection between source and first wall, which would be a disruption in reality, would produce completely wrong results in the programme, so it is very important that the source is well placed.

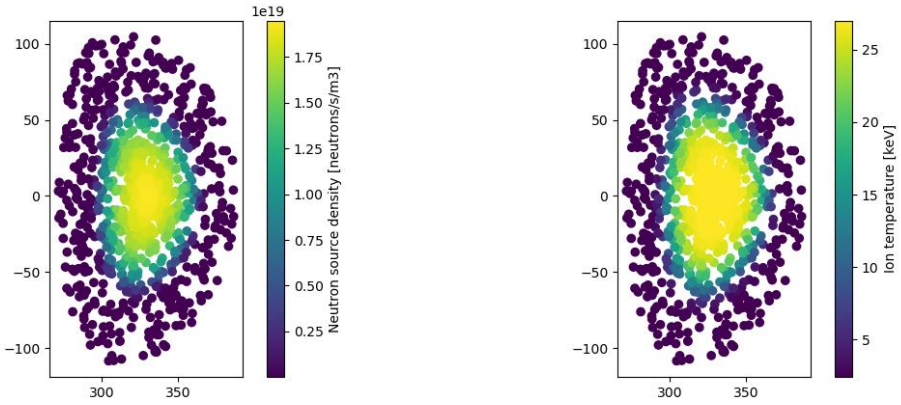

Fig. 2.9: *Neutron source density profile of the plasma (left), ion temperature profile (right).*

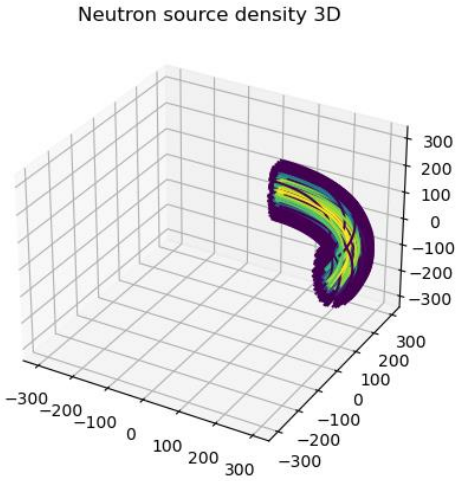

Fig. 2.10: *Three-dimensional view of the source.*

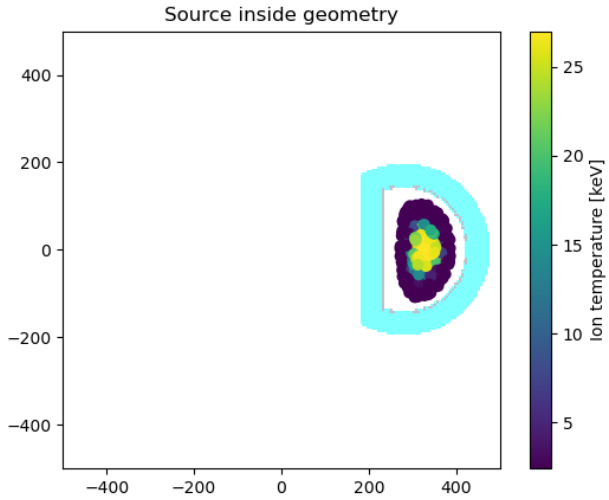

Fig. 2.11: *Cross section of the source located inside the D model: ion temperature representation.*

2.3.2 Inconel-718 as structural material

This high strength alloy is designed to resist a wide range of severely corrosive environments, pitting and crevice corrosion.

The chemical composition of Inconel-718 is shown in the Table 2-1.

The results shown in this paragraph are obtained considering 50000 particles divided in 30 batches plus 10 inactive batches.

Two tests are conducted: one using the beryllium layer as a neutron multiplier (as designed), and one removing it to verify the feasibility of removing it in reality.

Beryllium is a good material from the neutron point of view but is at the same time toxic, very difficult to handle (because it is powdered) and is extremely volatile. In addition, it is very expensive, so its removal would lead to a reduction in the cost of building the reactor. From the point of view of activation, it is a very bad component because it contains traces of impurities inside it among which the worst is uranium. This element once irradiated produces highly radioactive isotopes with very long half-lives such as plutonium-239.

Therefore, in the simulation without beryllium the thickness of the cooling channel is increased by one centimetre, to try to compensate for a lower neutron flux.

As shown from the results of the simulations in Fig. 2.12 and Fig.2.13, the removal of the neutron multiplier leads to a decrease in the production of tritium.

The idea of increasing the cooling channel proved to be excellent, because in that region of space the production of tritium remained almost the same, while in the outdoor tank there is a decrease.

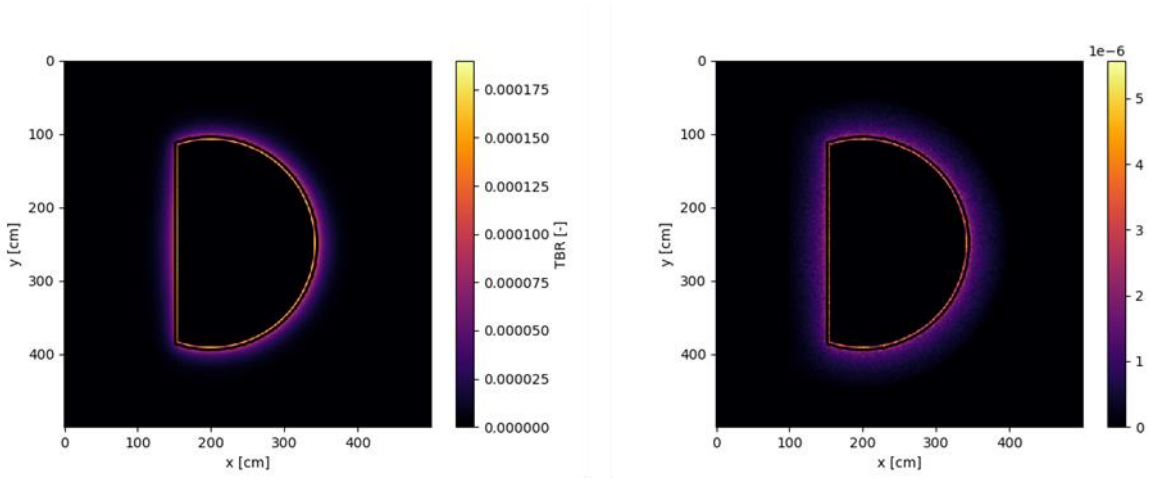

Fig. 2.12: *Tritium generation mesh tally mean result (left) and standard deviation (right) with Be layer.*

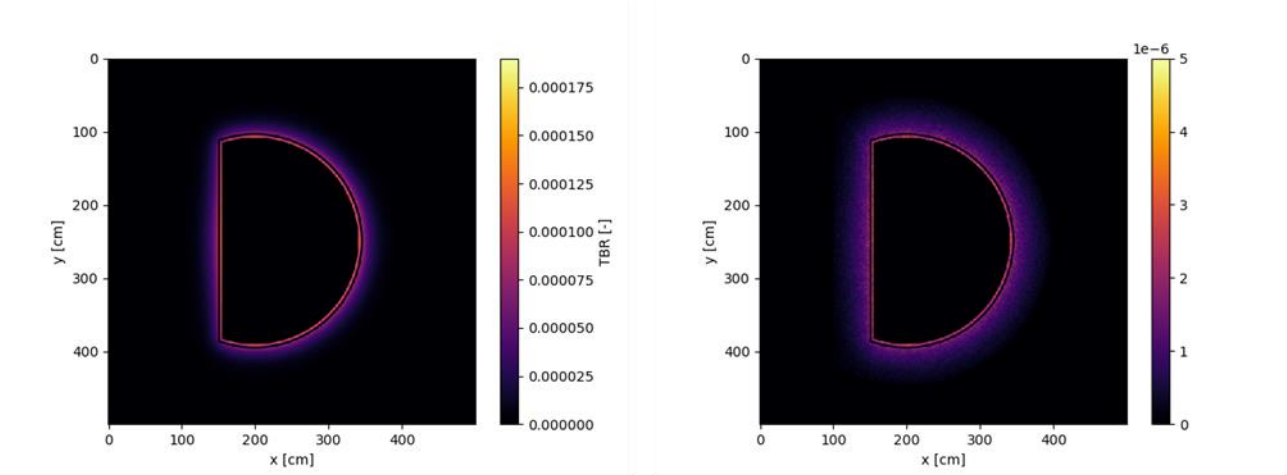

Fig. 2.13: *Tritium generation mesh tally mean result (left) and standard deviation (right) without Be layer.*

Table 2-5 *Tritium production fraction in each layer.*

Layer and configuration	TBR [-]	Standard deviation
Channel with Be layer	0.249	4.50e-04
Channel without Be layer	0.246	4.49e-04
Tank with Be layer	0.811	7.97e-04
Tank without Be layer	0.751	9.08e-04
Total with Be layer	1.060	1.25e-03
Total without Be layer	0.997	1.36e-03

The neutron flux is the most important quantity together with the TBR to evaluate; the reaction rate depends on the latter. Due to the absence of beryllium, there is a decrease in neutron flux, which leads to a decrease of the TBR. The decrease in flux does not lead to major changes in the cooling channel but rather in the pool of FLiBe surrounding the vacuum vessel.

The fewer neutrons arrive in the tank, the fewer type reactions (n, Xt) take place.

From the point of view of leakage, the values remain low and acceptable, therefore the decrease of 50 cm of the pool was a good evaluation. This data also does not affect the production of tritium as most of the reactions occur up to 20-30 cm from the vacuum vessel.

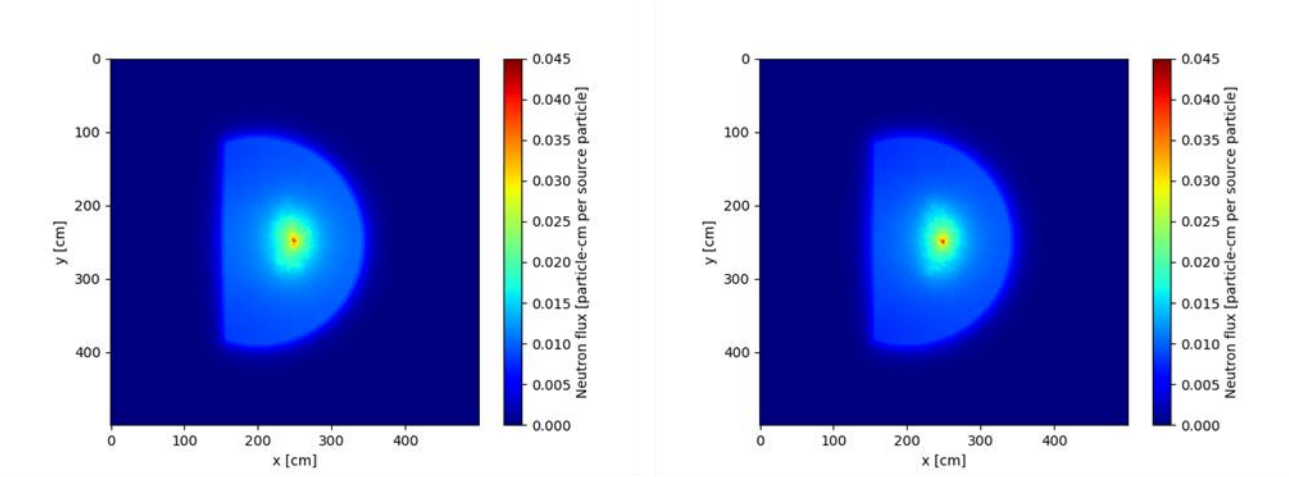

Fig. 2.14: *Neutron flux distribution on VV with Be as neutron multiplier (on the left) and without (on the right).*

2.3.3 High-entropy alloys as structural material

The simulation previously performed is repeated by replacing Inconel-718 with the proposed high-entropy alloy based on vanadium, chromium, tungsten, tantalum and titanium.

These elements are selected because: they are refractory (they withstand high temperatures), they are high-activation, some of them are well resistant to corrosion and have good radiation resistance. Alloys composed by vanadium, chromium and titanium have already been studied and have been shown to form low activation alloys [16].

However, the addition of tungsten increases the alloy's properties at high temperature, such as: oxidation resistance, mechanical strength, fracture resistance and toughness [23].

A sensitivity analysis is conducted by varying the composition of the alloy changing the amount of each element. In particular, an attempt is made to lower the chromium since it weakens the alloy being corroded by the molten salt and also the titanium is lowered because it makes the alloy fragile.

Having reduced the titanium content, efforts are made to increase the vanadium content in order to lighten the alloy. Tantalum is maintained in a good percentage because it is very resistant to corrosion, especially to the attack of acids, and it is a good heat conductor. Whereas in the G alloy it is tried to maximise the tungsten content, resulting in a significant increase in the density of the alloy.

In these simulations the beryllium layer has not been inserted, because unlike Inconel-718 this new alloy contains tungsten which has an excellent (n, 2n) cross section, even higher than that of beryllium.

Table 2-6 *High-entropy alloys chemical composition by wt%.*

Element composition	V	Cr	W	Ta	Ti	Density [g/cm^3]
Basic alloy	20	20	20	20	20	10.73
A	30	10	40	10	10	12.36
B	40	5	40	10	5	12.39
C	60	5	20	10	5	9.76
D	20	5	60	10	5	15.02
E	30	10	30	20	10	12.11
F	30	5	30	30	5	13.19
G	20	2.5	70	5	2.5	15.82

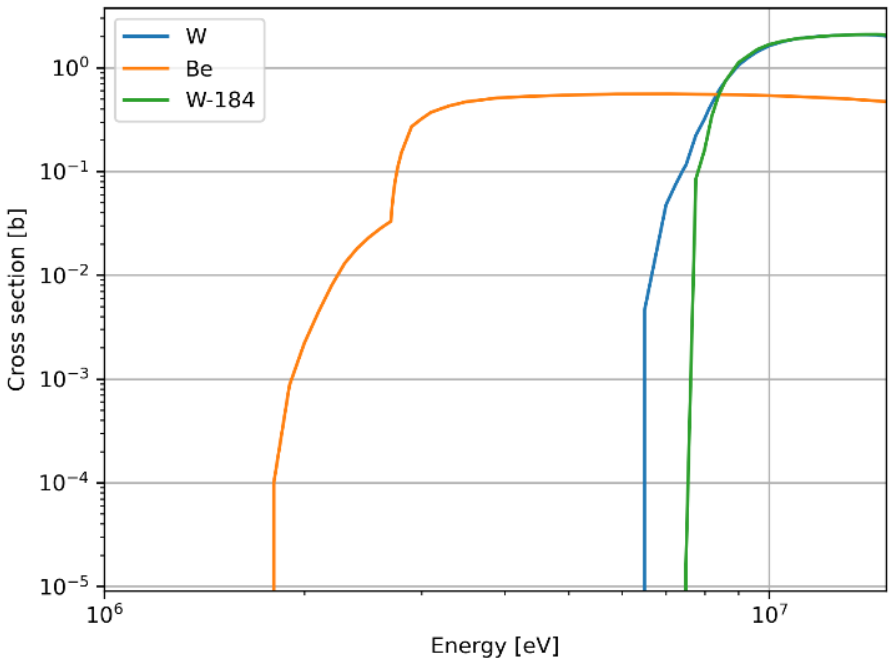

Fig. 2.15: *Neutron multiplication cross section of Be, W and W-184.*

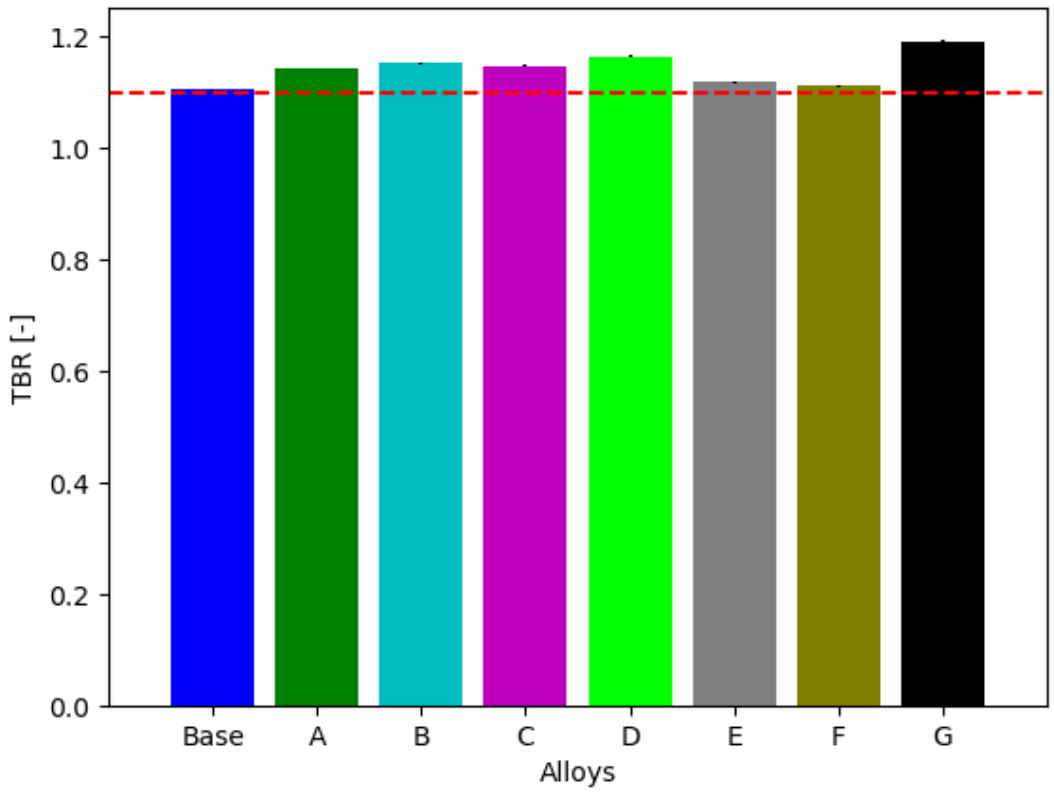

Fig. 2.16: *Tritium breeding ratio obtained with the eight tested alloys (the red line represent the value 1.1).*

Each proposed composition meets the minimum requirement for TBR.

Table 2-7 *Tritium breeding ratio obtained with the eight tested alloys*

Alloy	TBR [-]	Standard deviation
Base	1.105	1.21e-03
A	1.143	1.31e-03
B	1.152	1.33e-03
C	1.148	1.21e-03
D	1.164	1.31e-03
E	1.119	1.23e-03
F	1.112	1.23e-03
G	1.192	1.19e-03

The best in this respect are D and G alloys, which contain the largest amount of W, therefore a higher concentration of tungsten in the HEA leads to an increase in production of tritium.
Another aspect that emerges is that the less vanadium fits into the alloy, the greater will be the TBR. Regarding the concentration of chromium, tantalum and titanium what emerges from this study is that the less they are present the higher the TBR will be. The parameter that most influences the tritium breeding ratio turns out to be the concentration of tungsten.
The G alloy is the most interesting one, as it allows obtaining a really high TBR.

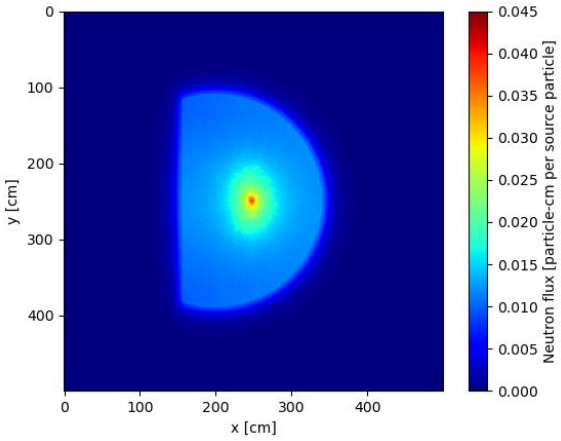

Fig. 2.17: *Neutron flux distribution on high-entropy alloy G.*

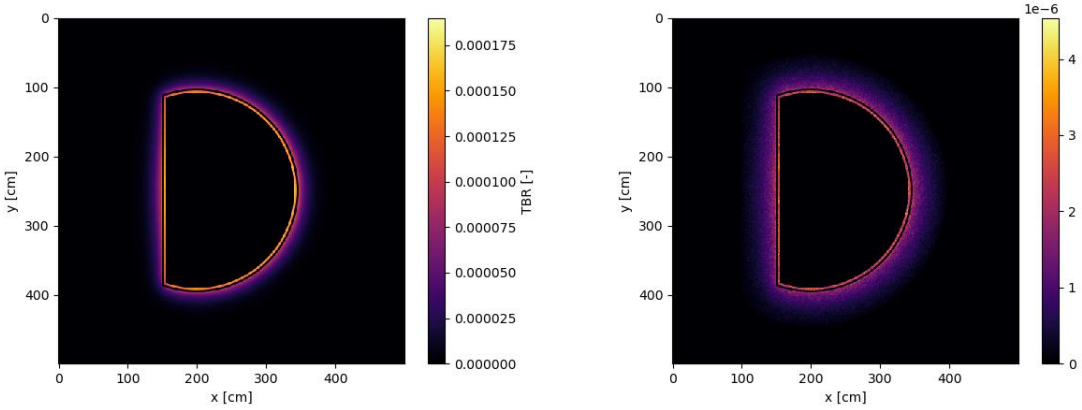

Fig. 2.18: *Tritium generation mesh tally mean result (left) and standard deviation (right) with HEA G.*

2.4 D-shape model with reflector

A tungsten carbide (WC) reflector with a thickness of 20 cm, is inserted outside the FLiBe tank. This simulation is carried out both for the case with Inconel-718 without the neutron multiplier and for the high-entropy alloy G.

The aim of this study is to see whether omitting beryllium but inserting a reflector would increase the TBR value.

The intention is to be able to insert a material with physical characteristics such as to make it suitable for reflecting neutrons by means of consecutive elastic shocks. This reflection pushes the neutrons into the FLiBe tank and increases the rate of reactions (n, Xt) in order to increase the tritium breeding ratio.

From the simulation it emerges that with a reflector positioned outside, the TBR increase of about 0.8%. It is not convenient to adopt such a technology since the expense to realise the shielding turns out superior to the gain.

In the case of Inconel-718, despite the leakage value was already excellent, the TBR without the Beryllium layer was insufficient, so this new solution leads to improvements even if minimal, since the final TBR obtained from the simulation is still less than 1.1.

2.5 Isotopic tailoring

This procedure consists in varying in an element the percentage of a particular isotope that composes it.

In particular, the choice is made to vary the presence of the isotope 184 within tungsten, since it is much less absorbent.

In addition, it is bought already enriched in W184.

Isotopic tailoring process is made for A, C and G alloys, which are interesting in some respects:

Table 2-8 *Isotopes of tungsten [24].*

Isotope	Abundance in nature
W-180	0.12
W-182	26.50
W-183	14.31
W-184	30.64
W-186	28.43

Of these isotopes the important one is the 180W which is radioactive and through an alpha decay leads to the formation of hafnium 176, which turns out to be an excellent neutron absorber. Fortunately, the presence of 180W is minimal.

Using OpenMC, natural tungsten is inserted as an element and the percentage of enrichment of nuclide W-184 is varied.

The percentage variation is made to vary from a 40% up to a 100% increasing it each time by a 10%.

From A alloy it is obtained a growing trend with the increase of 184W, in particular there is a percentage variation of about 0.86%.

Same for C alloy, where the percentage variation is about 0.60%.

For G alloy the percentage variation is 2.23%.

In conclusion, increasing the presence of the nuclide W-184 in the high entropy alloy results in an increase in TBR. As can be seen from Fig.2.15 showing the neutron multiplication cross section, the W-184 has the same qualities as the natural high-energy W.

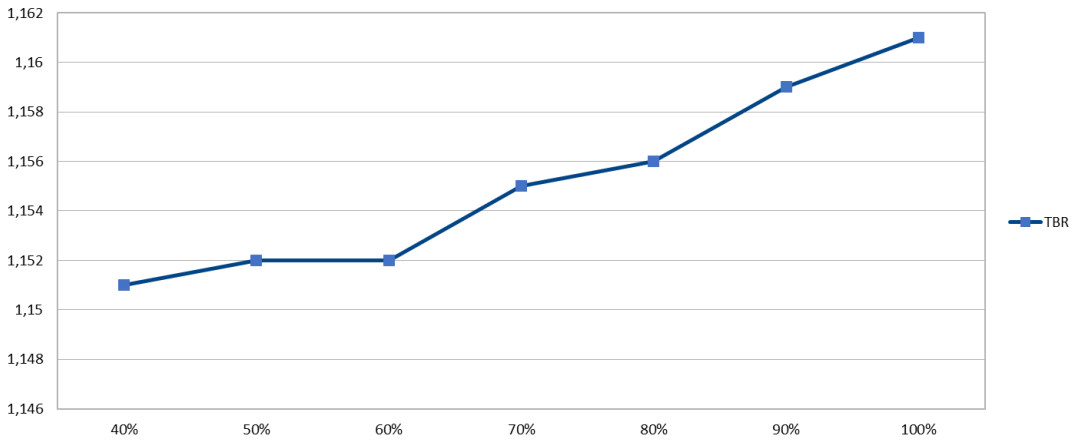

Fig. 2.19: *Isotopic tailoring: alloy A, TBR.*

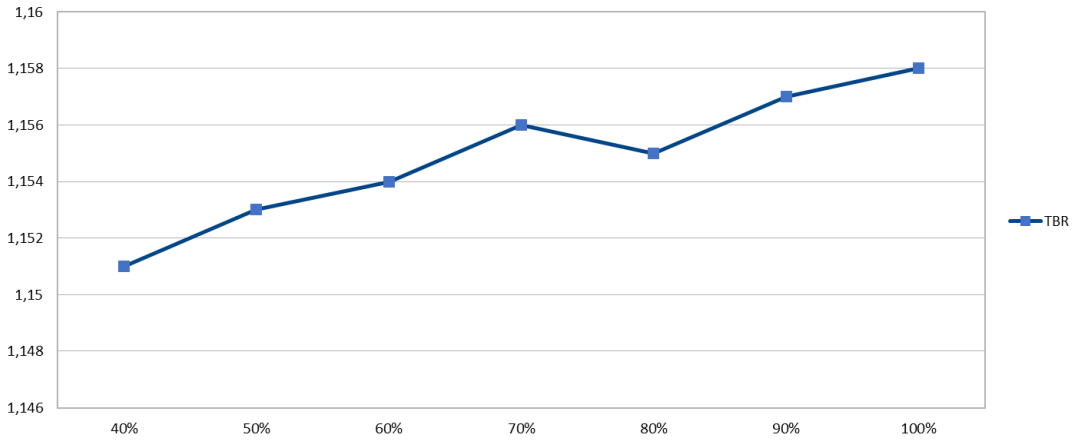

Fig. 2.20: *Isotopic tailoring: alloy C, TBR.*

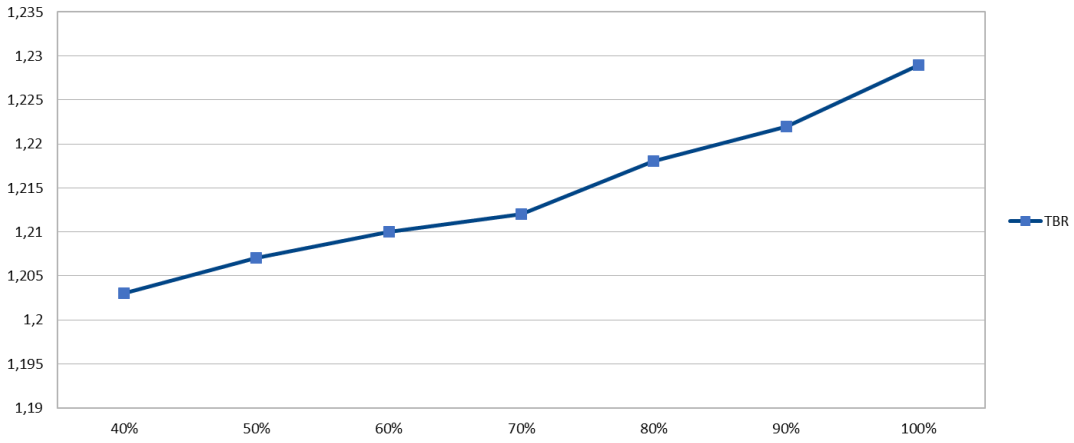

Fig. 2.21: *Isotopic tailoring: alloy G, TBR.*

Chapter 3

3 Activation analysis

This chapter examines the problem of neutron induced radioactivity in ARC structural materials.

In particular, three different compositions of the proposed high entropy alloy are analysed by comparing them with Inconel-718. The FISPACT-II program simulates the exposure of pure materials and checks whether the radioactivity induced in these materials is such that they can be classified as 'low activation'. To define the notion of low activity, two concepts are considered: recycling and confinement in controlled surface deposits.

In particular, the limits that have been proposed in paragraph 3.2 that refer to the limits within 100 years from the shutdown of the plant or the disposal of a component must be respected.

Finally, after demonstrating the improvement aspects involved in the use of a high entropy alloy compared to Inconel-718, the exposure of materials containing the minimum content of impurities now achievable is simulated.

3.1 FISPACT-II

FISPACT-II is an inventory code capable of performing modelling of activation, transmutations and depletion induced by neutron, proton, alpha, deuteron or gamma particles incident on matter [25]. FISPACT-II possesses many features but the most common simulations are performed with time-dependent inventories, observables and emitted particle data.

The code operates in four stages: first process the library data, secondly set initial conditions, thirdly run irradiation (heating) phases and finally run cooling phases.

This program needs 6 input files to work: collapse.i, condense.i, inventory.i, print_lib.i, files and fluxes. The most important are the inventory.i files, which contains the detailed description of the material being irradiated and fluxes, since it contains the neutron flux with which the material is irradiated.

3.2 Neutron induced activation

The International Atomic Energy Agency (IAEA) in 2009 published a classification of radioactive waste into 6 different classes [26].

Waste produced in ARC should be classified as low-level waste, that means it is above permit levels but with limited quantities of long-lived radionuclides.

Contact radiation dose rate is not used to distinguish waste classes in the new IAEA classification scheme. The guide assumes that detailed quantitative boundaries taking into account broad range of parameters may be developed in accordance with national programs and requirements.

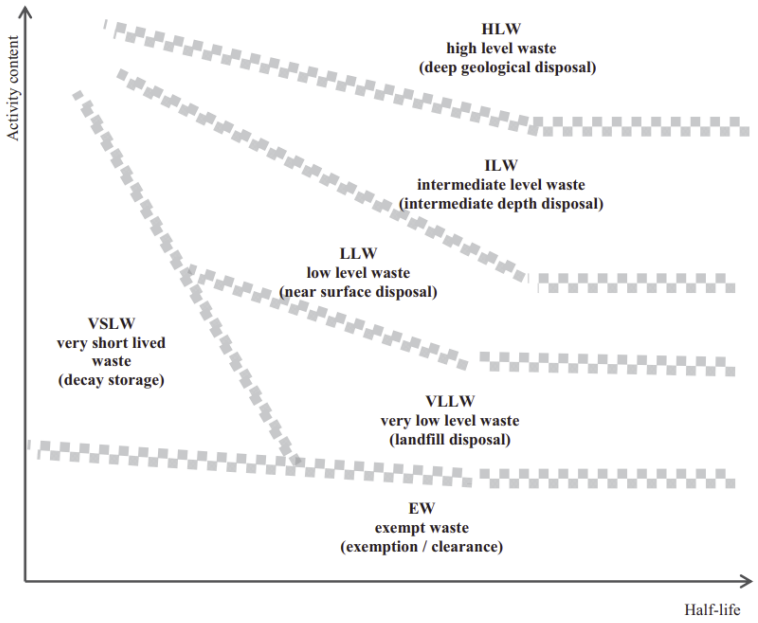

Fig. 3.1: *Conceptual illustration of the waste classification scheme [26].*

Nevertheless, limits have been adopted in ARC to understand how to recycle/reuse the components and materials discharged; in particular, four options have been proposed [3]:

- Outside the nuclear industry (dose rate of 1e-5 Sv/h as reference)
- Within the nuclear industry or in general industry for specific applications (dose rate of 1e-6 Sv/h)
- In a landfill (dose rate of 1.14e-7 Sv/h as reference to the natural background average dose)
- The material can be recycled if its clearance index has returned equal to 1.

"Clearance" (unrestricted release from regulatory control) means that material complying with the requirements defined by national regulatory authorities may be managed as if it did not contain radioactivity higher than that present in nature [27].

Under this option, the material can be reused, recycled or disposed of in any landfill. The main requirement for unconditional reclamation is that the CI index is lower than the unit.

Evaluated with the following formula:

$$CI = \sum_{i}^{\#\,isotopes} \frac{A_i}{L_i} \tag{3.1}$$

A_i and L_i are the specific activity [Bq/kg] and the clearance limit for the i-th isotope contained in the material [27].

The limits proposed above are intended to be reached within 100 years from the disposal of a component, but for ARC have been proposed shorter times, which are presented in the following table.

Table 3-1 *Main recycling limits for fusion radioactive waste [3].*

Limits	Generic goals	ARC goals
In-plant recycling	100 years	10 years
Out-plant recycling	100 years	50 years
Clearance Index	100 years	100 years

To evaluate the activation, the program FISPACT-II is used simulating the hardest condition for ARC: one full power year with a neutron flux of 7-8e+14 n/cm2/s, as was also done in the paper [3]. Spectra and fluxes are derived from the earlier study of neutronics with OpenMC.

In particular, the obtained data is processed in order to build the file "fluxes" which is a fundamental input of FISPACT-II.

The results obtained as output are processed with MATLAB in order to be able to plot activity, dose rate and heat output.

The neutron fluxes in the first layer of structural material are shown in Fig3.2.

The neutron flux has been computed with 709 energy groups, as requested by FISPACT-II.

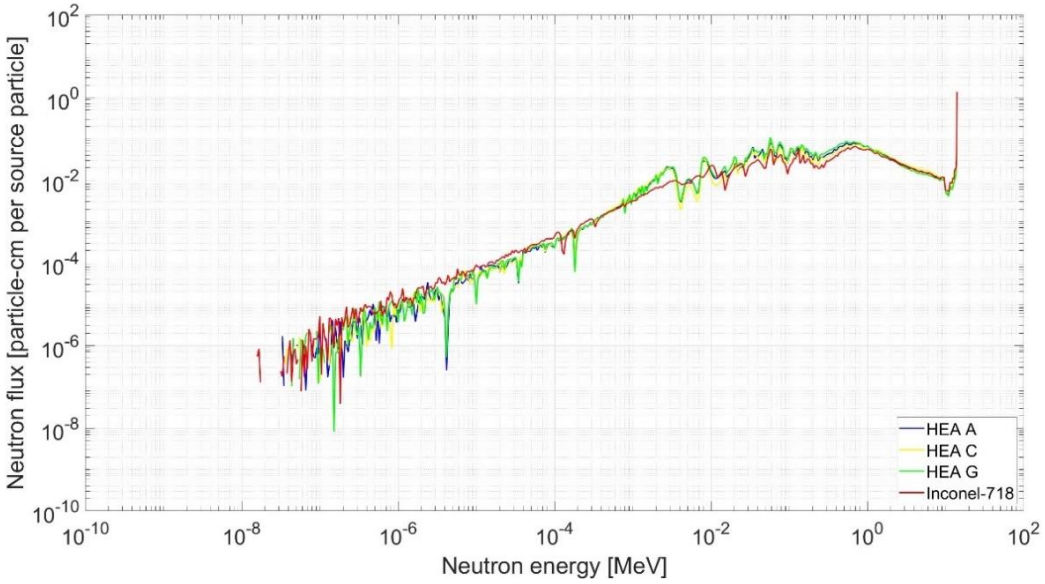

Fig. 3.2: *Neutron spectra in STR1.*

3.2.1 Pure materials: comparative results

Inconel-718 has been proposed for its good mechanical properties and chemical resistance at very high temperatures.

The high entropy alloy is proposed as a low activation material and is studied in its basic composition and in the proposed variants A, C and G (the same in which isotopic tailoring was made). In the following graphs it is proposed a comparison between the use of Inconel-718 and that of high entropy alloys in order to highlight the behaviour of the latter to neutron activation.

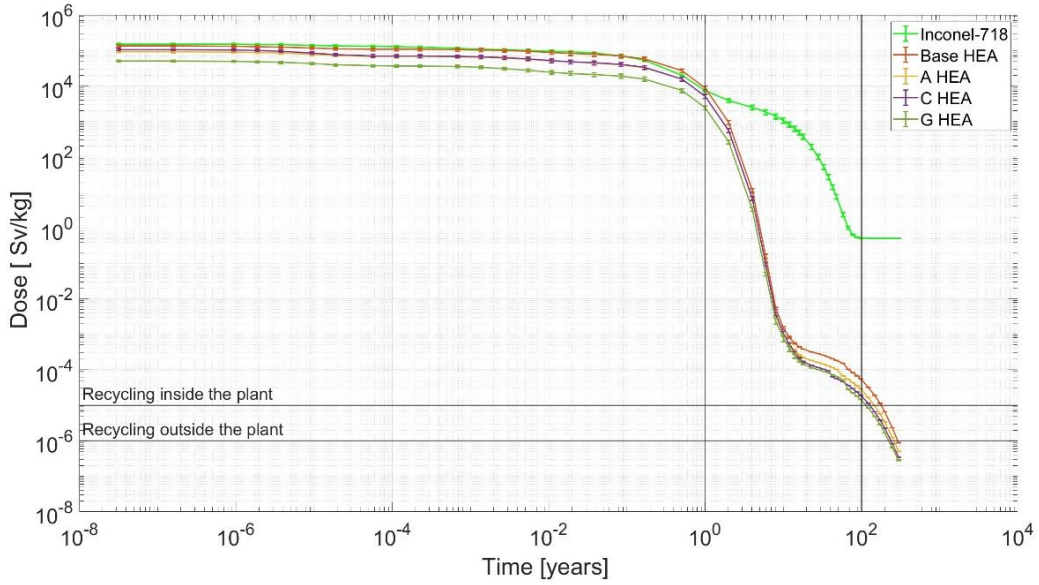

Fig. 3.3: *Comparison between Inconel-718 and HEAs: specific dose.*

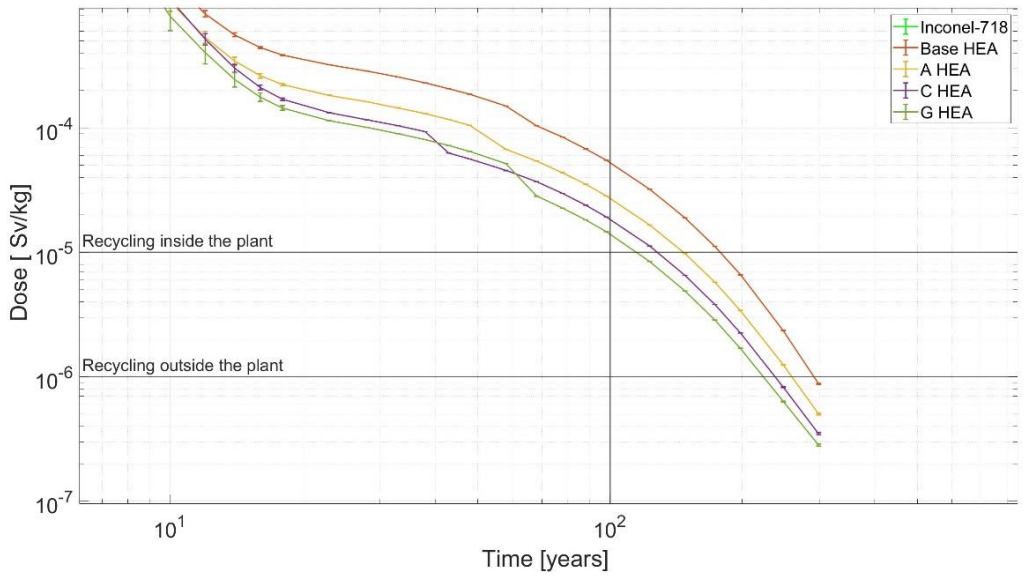

Fig. 3.4: *Comparison between Inconel-718 and HEAs: specific dose (zoom in).*

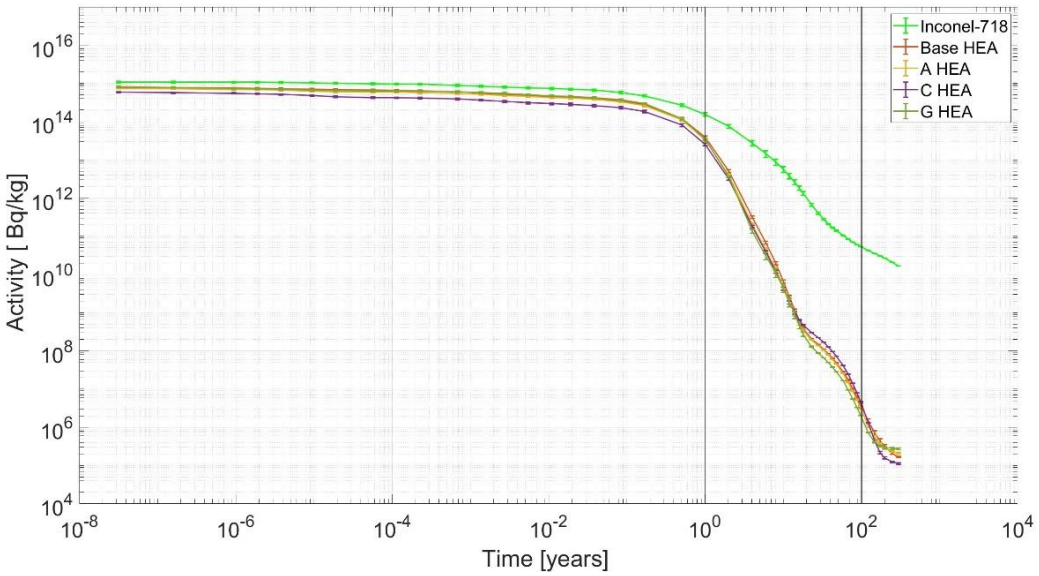

Fig. 3.5: *Comparison between Inconel-718 and HEAs: specific activity.*

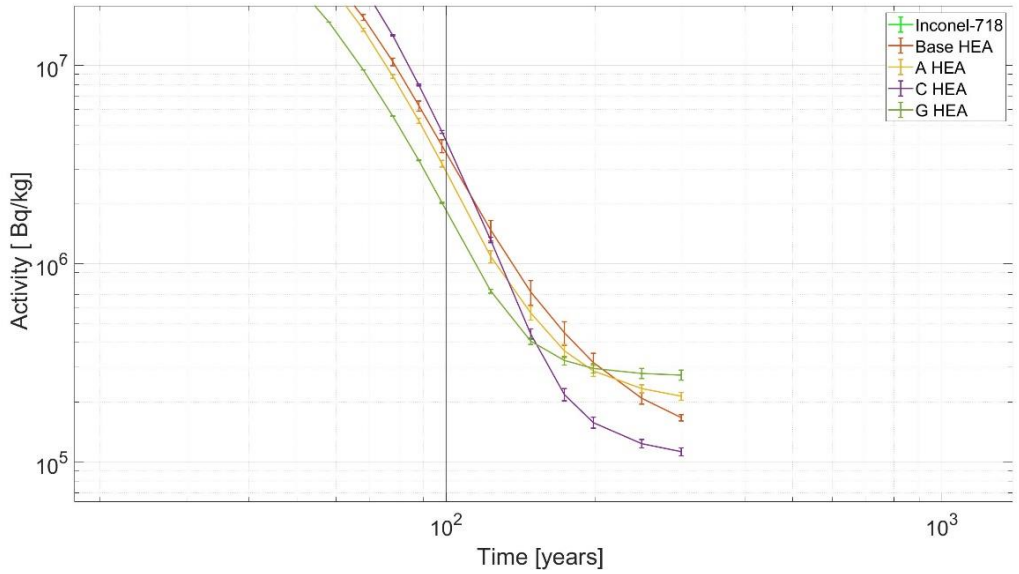

Fig. 3.6*: Comparison between Inconel-718 and HEAs: specific activity (zoom in).*

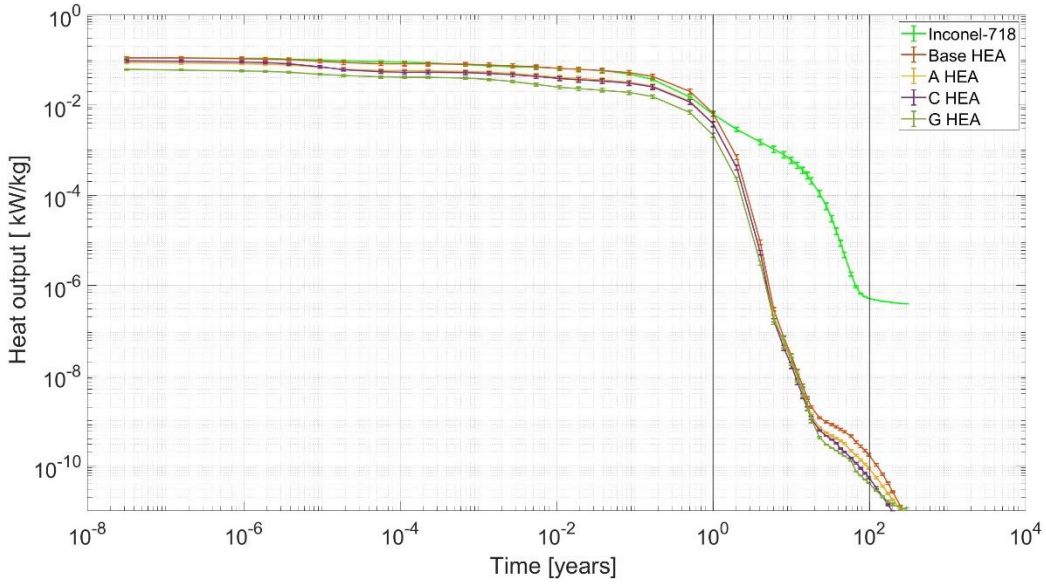

Fig. 3.7: *Comparison between Inconel-718 and HEAs: specific heat output.*

The dose rate is quantity of radiation absorbed or delivered per unit time.

What emerges from this comparison is that the new alloy in the four compositions under consideration is much better than Inconel-718. It almost manages to meet the recycling limit within the plant.

Inconel-718, furthermore, causes a high inventory of radioactive materials.

Nickel is the main cause of such high radioactivity. Its main products have a long-half life and the dose rate stabilises at about five orders of magnitude more than any recycling limit [5].

It can be seen from Fig.3.4 that after 100 years, G alloy allows for lower dose levels than the others examined here. This is due to the presence of titanium in the alloy. Titanium when irradiated leads to the formation of Ar-42, a radionuclide characterized by β^- decay. A perfect tailoring of Ti-50 would prevent the formation of noble gas Ar-42 and, therefore, its high-energy decaying daughter K-42 [3].

The activity is defined as the number of radioactive transformation per second per kg.

The graph shows that G alloy reaches the lowest activity levels, as it turns out to be the alloy that absorbs the least radiation. However, in times over 100 years, C alloy achieves lower levels of activity.

The heat output is the heat generated by the decay of radionuclides. Its analysis is important for what concerns waste management, because high heat waste is more difficult to manage and requires higher operating costs.

Obviously, at lower activity levels there are lower heat levels, therefore the trend is consistent with that of the activity. The result is that in 100 years G alloy is the best, followed by C alloy, A alloy and then the base. Instead, in times over 100 years, C alloy is confirmed the best.

3.3 Impurity analysis

Impurities are by definition a qualitative alteration, consisting of the presence of foreign elements. When an alloy is created within it, impurities are trapped from the process itself used for its creation and from the impurities that were already present in the elements that constitute it. Since the proposed high entropy alloy is irradiated, it is important to understand and study what impurities are present in it, in what concentration and how they modify the behaviour of the alloy.

The Table 3-2 containing the impurities characterising the V-Cr-Ti alloy, tantalum and tungsten, are shown in Table 3-3 and Table 3-4. Finally, Table 3-6 incorporates all these impurities and associates them with each of the alloys studied.

Table 3-2 *V-Cr-Ti impurities [3].*

Impurity	ppm on the element	% on the element
C	0.05	0.000005
N	0.1	0.00001
O	0.2	0.00002
Al	0.1	0.00001
Si	0.3	0.00003
Fe	0.1	0.00001
Ni	0.01	0.000001
Cu	0.005	0.0000005
Nb	0.001	0.0000001
Mo	0.025	0.0000025
Te	0.05	0.000005

Table 3-3 *W impurities [28].*

Impurity	ppm on the element	% on the element
O	5	0.0005
N	5	0.0005
C	5	0.0005
Na	0.1	0.00001
K	0.05	0.000005
Al	0.05	0.000005
Ca	0.2	0.00002
Cu	0.05	0.000005
Fe	15	0.0015

Table 3-4 *Ta impurities [29].*

Impurity	ppm on the element	% on the element
Pb	0.14	0,000014
Th	0.11	0.000011
U	0.17	0.000017
Al	2.15	0.000215
Mn	0.12	0.000012
Co	0.72	0.000072
Ni	8.35	0.000835
Cu	0.35	0.000035
Zn	0.32	0.000032
Sr	0.07	0.000007
Zr	29.3	0.00293
Nb	18.3	0.00183
Mo	4.2	0.00042
Ag	0.52	0.000052
Cd	0.1	0.00001
Ba	0.11	0.000011
Hf	0.5	0.00005

Table 3-5 *High-entropy alloys main element composition.*

Alloy	Base	A	C	G
V	19.9999812	29.9999843	59.999978	19.9999922
Cr	19.9999812	9.99998432	4.99997804	2.49999216
W	19.999391	39.998782	19.999391	69.9978685
Ta	19.9986894	9.9993447	9.9993447	4.99967235
Ti	19.9999812	9.99998432	4.99997804	2.49999216

Table 3-6 *Total impurities on each alloy wt%.*

Impurity	Base	A	C	G
Pb	0.0000028	0.0000014	0.0000014	0.0000007
Th	0.0000022	0.0000011	0.0000011	0.00000055
U	0.0000034	0.0000017	0.0000017	0.00000085
Al	0.00005	0.0000285	0.0000295	0.00001675
Mn	0.0000024	0.0000012	0.0000012	0.0000006
Co	0.0000144	0.0000072	0.0000072	0.0000036
Ni	0.0001676	0.000084	0.0000842	0.000042
Cu	0.0000083	0.00000575	0.00000485	5.375E-06
Zn	0.0000064	0.0000032	0.0000032	0.0000016
Sr	0.0000014	0.0000007	0.0000007	0.00000035
Zr	0.000586	0.000293	0.000293	0.0001465
Nb	0.00036606	0.00018305	0.00018307	9.1525E-05
Mo	0.0000855	0.00004325	0.00004375	2.1625E-05
Ag	0.0000104	0.0000052	0.0000052	0.0000026
Cd	0.000005	0.0000035	0.0000045	0.00000175
Ba	0.0000022	0.0000011	0.0000011	0.00000055
Hf	0.00001	0.000005	0.000005	0.0000025
O	0.000112	0.00021	0.000114	0.000355
N	0.000106	0.000205	0.000107	0.0003525
C	0.0001	0.0002	0.0001	0.00035
Na	0.000002	0.000004	0.000002	0.000007
K	0.000001	0.000002	0.000001	0.0000035
Ca	0.000004	0.000008	0.000004	0.000014
Fe	0.000306	0.000605	0.000307	0.0010525
Si	0.000018	0.000015	0.000021	0.0000075
Te	0.000003	0.0000025	0.0000035	0.00000125

The mostly present impurity turns out to be the Niobium, however it is not a huge problem since if irradiated it leads to the formation of stable molybdenum. Other impurities, namely uranium and nickel (which is responsible for the activation of Inconel-718) cause problems because these elements once irradiated produce highly radioactive isotopes with a very long half-life that are damaging for the system.

3.3.1 High-entropy alloy G

Since G alloy has been shown to be the best in terms of allowing tritium production and neutron induced activation, it is analysed to see how it varies with the presence of impurities when irradiated with neutron flux.

The Fig.3.8, Fig.3.9 and Fig.3.10 show that the presence of impurities results in a higher dose rate and consequently an increase in activity and decay heat.

However, this increase is not significant even if it is far from the dose rate value needed to recycle materials inside the nuclear plant.

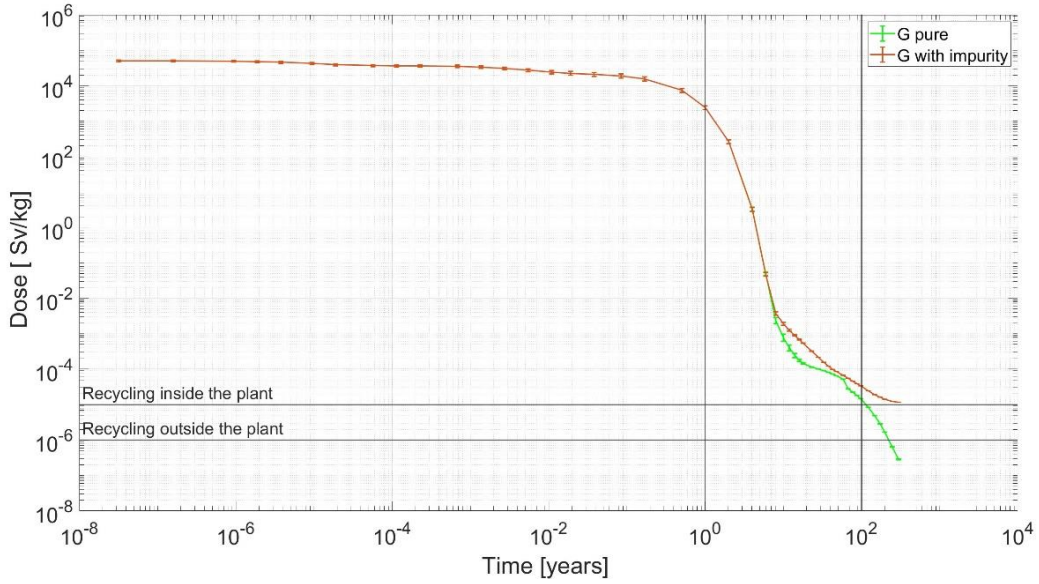

Fig. 3.8: *High-entropy alloy G pure and with impurities: specific dose.*

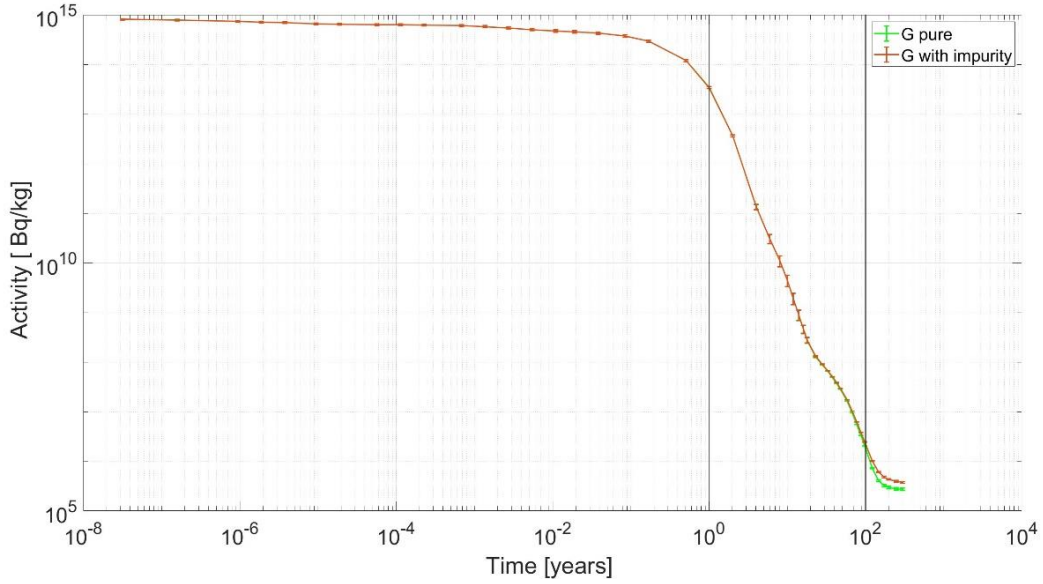

Fig. 3.9: *High-entropy alloy G pure and with impurities: specific activity.*

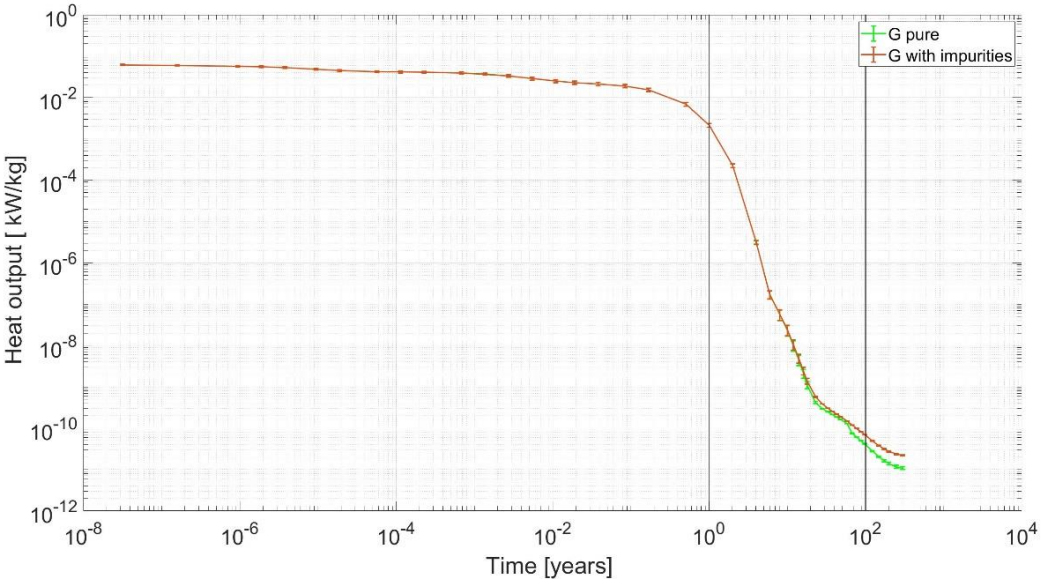

Fig. 3.10: *High-entropy alloy G pure and with impurities: specific heat output.*

3.3.2 Materials with impurities: comparative results

In the following images were plotted the trends of the 4 alloys in question compared with the pure Inconel-718.

It emerges that, despite the presence of impurities adversely affects the performance of high entropy alloys causing an increase in dose rate and moving the values away from the limits to be respected, after 100 years, it is about 4 orders of magnitude better than the Inconel-718.

Among the high entropy alloys, G alloy is always the best, as it has a much lower percentage of uranium and nickel as impurities than the others.

Actually, uranium and nickel are impurities that are mostly contained in tantalum, but this alloy has a tantalum composition that is half of A and C alloys and a quarter of the base alloy.

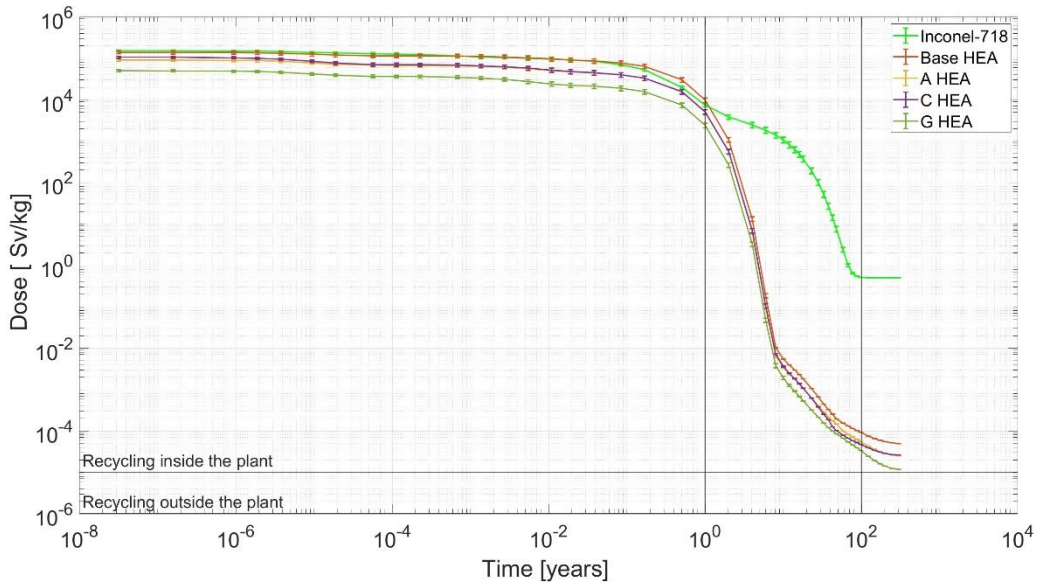

Fig. 3.11: *Inconel-718 vs. High-entropy alloys with impurities: specific dose.*

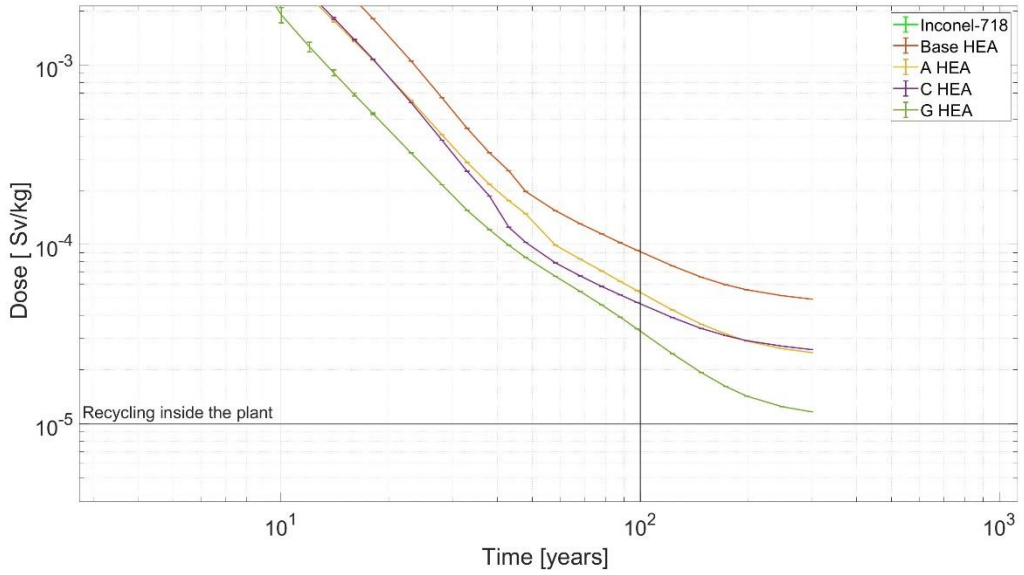

Fig. 3.12: *Inconel-718 vs. High-entropy alloys with impurities: specific dose (zoom in).*

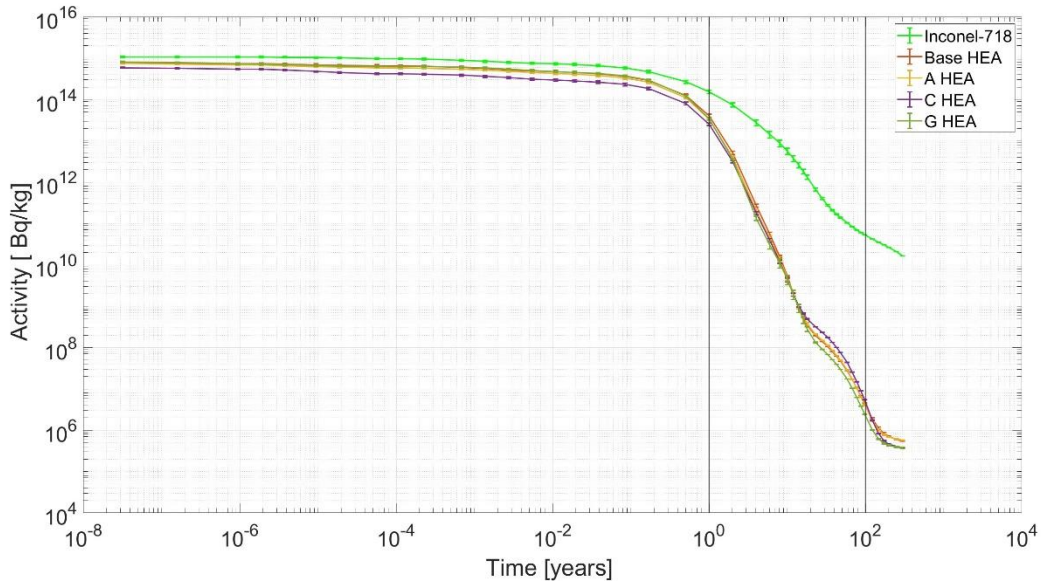

Fig. 3.13: *Inconel-718 vs. High-entropy alloys with impurities: specific activity.*

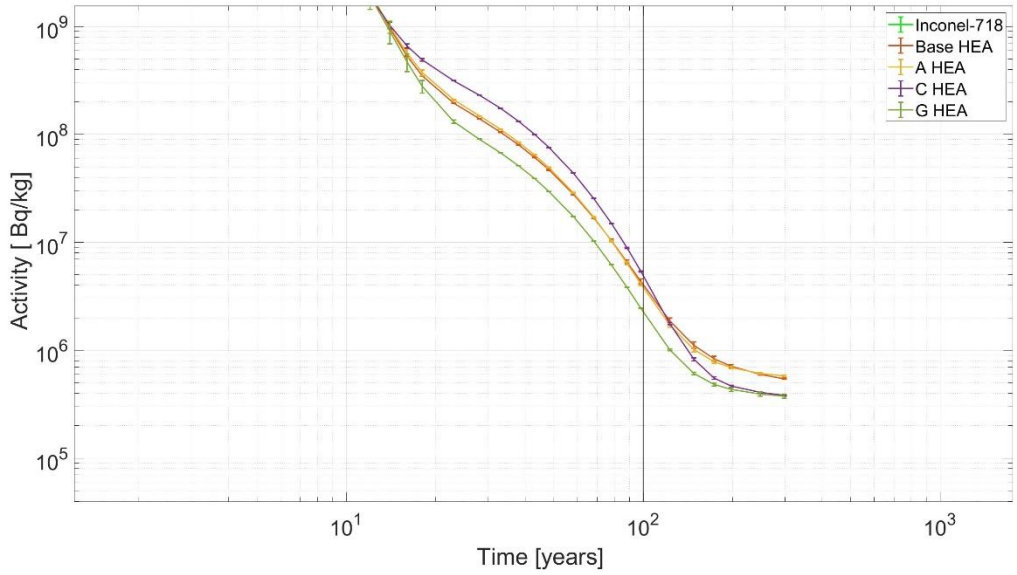

Fig. 3.14: *Inconel-718 vs. High-entropy alloys with impurities: specific activity (zoom in).*

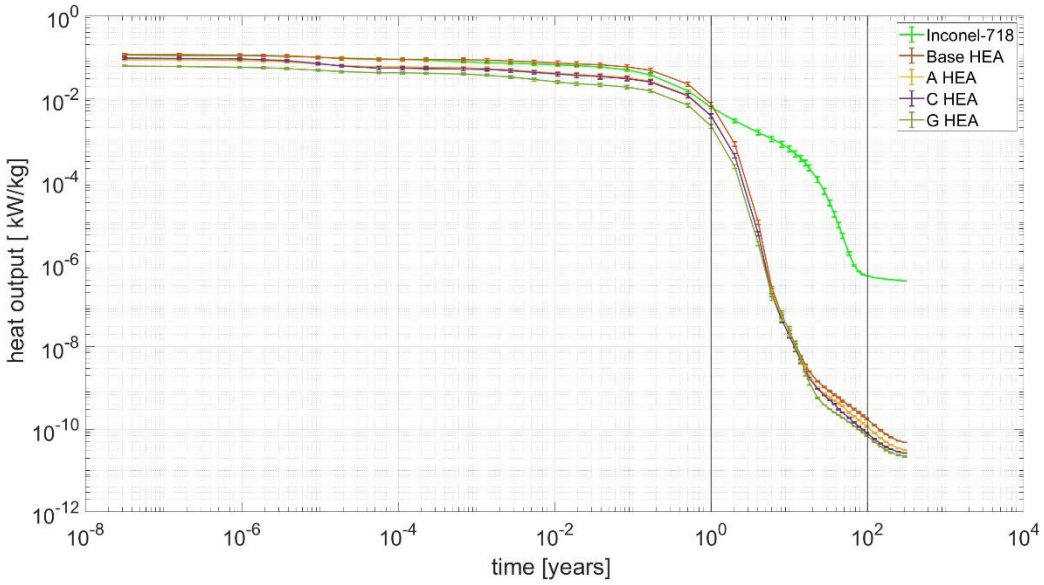

Fig. 3.15: *Inconel-718 vs. High-entropy alloys with impurities: specific heat output.*

Chapter 4

4 Conclusion

The main goal of this research is the study of a new material suitable to replace Inconel-718 as structural material for the vacuum vessel. This study shows the limitations that the use of Inconel-718 entails with regard to the tritium breeding ratio and especially for activation.

The new high entropy alloy consisting of vanadium, chromium, titanium, tantalum and tungsten has proven to be highly performing from a neutronics point of view, so that a TBR of 1.1 can be achieved by omitting the neutron multiplier layer made of beryllium.

The possibility of removing this layer is a significant step forward in the activation of materials and their disposal, as well as increasing the acceptance by the population of this new technology.

In addition to the excellent results found in the neutronic field, this new alloy and its variants that have been proposed have demonstrated the almost possibility of recycling in about a century inside the plant, especially the G alloy which is therefore the best both from the neutron and the activation point of view.

G alloy is the proposed one with the highest tungsten content: it was composed of 70% W, 20% V, 5% Ta, 2.5% Cr and 2.5% Ti.

The presence of impurities that can form inside the alloy during its creation has been shown to be relevant from the point of view of activation, dose rate and heat output, therefore, it is classified as a low-activation material.

The presence of impurities means that the time targets for disposal usually wanted by the fusion community are not met. Actually, after 100 years the dose rate is higher than 1e-5 Sv/h, which is the limit to recycle them within the nuclear industry.

The results obtained are however excellent because, even if they do not allow this type of recycling, they guarantee very low levels of activity compared to those obtained with other materials.

For example, the high-entropy G alloy without impurities can achieve the dose requirement to ensure in-plant recycle in about 110 years. With the presence of impurities such a dose value is reached in about 300 years.

The objectives set by the designers of ARC to reach dose rate levels such as to ensure in-plant recycling after only 10 years, have not been achieved even by the alloys without impurities.

Studies that can still be done on this alloy are its behaviour at high temperatures and its resistance to high thermal loads. It is also interesting to analyse its resistance to corrosion, since, in ARC case study, it comes into contact with a molten salt: the FLiBe which is highly corrosive, therefore it is necessary to understand its strength and durability in such a complex environment.

A further analysis may concern the mechanical strength of these alloys. This may be very interesting because the G alloy has given the best results in every aspect analysed, but it has a density of about 1/3 greater than that of Inconel-718, therefore it will be important to understand how such an increase in weight can burden the plant and maintenance systems.

It is also interesting to understand the technological properties of this new high entropy alloy, and how they affect the particular processes that will have to undergo to build the vacuum vessel.

One last very important thing that should never be underestimated is a careful economic analysis. The alloy here analysed would bring many benefits, but we do not yet know how much its production can cost.

Appendix A

Example of code with OpenMC for D-shape model with high-entropy alloy.

```
import openmc
import matplotlib.pyplot as plt
from openmc_plasma_source import TokamakSource, plot_tokamak_source_3D,
scatter_tokamak_source
from plotly.offline import download_plotlyjs, plot
from plotly.graph_objs import Scatter, Layout

################################################################################
# Create materials for the problem
w = openmc.Material(name='Tungsten')  #first wall
w.add_nuclide('W184', 1.)
w.set_density('g/cm3', 19.250)
w.temperature = 900.0  # temperature in Kelvin

hea = openmc.Material(name='High-entropy alloy HEA')  #structural layers
hea.add_element('V', 0.2,'wo')
hea.add_element('Cr', 0.2,'wo')
hea.add_element('W', 0.2,'wo')
hea.add_element('Ta', 0.2,'wo')
hea.add_element('Ti', 0.2,'wo')
hea.set_density('g/cm3', 10.7314)
hea.temperature = 900.0

flibe = openmc.Material(name='FLiBe')  #breeding blanket (Li-6 enrichment 90 %)
flibe.add_element('F', 4.)
flibe.add_element('Be', 1.)
flibe.add_nuclide('Li6', 1.8)
flibe.add_nuclide('Li7', 0.2)
flibe.set_density('g/cm3', 1.94)
flibe.temperature = 900.0

be = openmc.Material(name='Berillium')  #neutron multiplier
be.add_element('Be', 1.)
be.set_density('g/cm3', 1.848)
be.temperature = 900.0

void = openmc.Material(name='Void')  #hydrogen to simulate vacuum
void.add_element('H', 1.0)
void.set_density('g/cm3', 0.0001)
void.temperature = 900.0
```

```
wc = openmc.Material(name='Tungsten Carbide')
wc.add_element('C', 1.)
wc.add_element('W', 1.)
wc.set_density('g/cm3', 15.63)
wc.temperature = 900.0

# Collect the materials together and export to XML
materials = openmc.Materials([w, hea, flibe, be, void, wc])
materials.export_to_xml()

################################################################################
# GEOMETRY

# high field side planes
hf_fw_inner = openmc.XPlane(x0=-42.9+330-50, name='hf fw inner')
hf_str1_inner = openmc.XPlane(x0=-43.0+330-50, name='hf str1 inner')
hf_channel_inner = openmc.XPlane(x0=-44.0+330-50, name='hf channel inner')
hf_nmult_inner = openmc.XPlane(x0=-46.0+330-50, name='hf nmult inner')
hf_str2_inner = openmc.XPlane(x0=-47.0+330-50, name='hf str2 inner')
hf_blanket_inner = openmc.XPlane(x0=-50.0+330-50, name='hf blanket inner')
hf_shield_inner = openmc.XPlane(x0=-100.0+330-50, boundary_type='vacuum',
                  name='hf shield inner')
#hf_shield_outer = openmc.XPlane(x0=-120.0+330-50, boundary_type='vacuum',
                  name="hf shield outer")

# low field side cylinders
lf_fw_inner = openmc.YCylinder(x0=330-50, z0=0, r=139.9, name='lf fw inner')
lf_str1_inner = openmc.YCylinder(x0=330-50, z0=0, r=140.0, name='lf str1 inner')
lf_channel_inner = openmc.YCylinder(x0=330-50, z0=0, r=141.0, name='lf channel inner')
lf_nmult_inner = openmc.YCylinder(x0=330-50, z0=0, r=143.0, name='lf nmult inner')
lf_str2_inner = openmc.YCylinder(x0=330-50, z0=0, r=144.0, name='lf str2 inner')
lf_blanket_inner = openmc.YCylinder(x0=330-50, z0=0, r=147.0, name='lf blanket inner')
lf_shield_inner = openmc.YCylinder(x0=330-50, z0=0, r=197.0, boundary_type='vacuum',
                  name='lf shield inner')
#lf_shield_outer = openmc.YCylinder(x0=330-50, z0=0, r=217.0, boundary_type='vacuum',
                  name='lf shield outer')

# Z planes
lower_bound = openmc.YPlane(y0=-50, boundary_type='reflective')
upper_bound = openmc.YPlane(y0=50, boundary_type='reflective')

# selecting regions
PLASMA = +hf_fw_inner & -lf_fw_inner & +lower_bound & -upper_bound
FW = ((-hf_fw_inner & +hf_str1_inner & -lf_str1_inner) |
                  (+lf_fw_inner & -lf_str1_inner & +hf_str1_inner)) &
                  +lower_bound & -upper_bound
STR1 = ((-hf_str1_inner & +hf_channel_inner & -lf_channel_inner) |
                  (+lf_str1_inner & -lf_channel_inner & +hf_channel_inner)) &
                  +lower_bound & -upper_bound
```

```
CHANNEL = ((-hf_channel_inner & +hf_nmult_inner & -lf_nmult_inner) |
                (+lf_channel_inner & -lf_nmult_inner & +hf_nmult_inner)) &
                +lower_bound & -upper_bound
NMULT = ((-hf_nmult_inner & +hf_str2_inner & -lf_str2_inner) |
                (+lf_nmult_inner & -lf_str2_inner & +hf_str2_inner)) &
                +lower_bound & -upper_bound
STR2 = ((-hf_str2_inner & +hf_blanket_inner & -lf_blanket_inner) |
                (+lf_str2_inner & -lf_blanket_inner & +hf_blanket_inner)) &
                +lower_bound & -upper_bound
BLANKET = ((-hf_blanket_inner & +hf_shield_inner & -lf_shield_inner) |
                (+lf_blanket_inner & -lf_shield_inner & +hf_shield_inner)) &
                +lower_bound & -upper_bound
#SHIELD = ((-hf_shield_inner & +hf_shield_outer & -lf_shield_outer) |
                (+lf_shield_inner & -lf_shield_outer & +hf_shield_outer)) &
                +lower_bound & -upper_bound

# creating cells
plasma = openmc.Cell(1, fill=void, name='plasma', region=PLASMA)
first_wall = openmc.Cell(2, fill=w, name='first wall', region=FW)
str1 = openmc.Cell(3, fill=hea, name='str1', region=STR1)
channel = openmc.Cell(4, fill=flibe, name='channel', region=CHANNEL)
nmult = openmc.Cell(5, fill=be, name='nmult', region=NMULT)
str2 = openmc.Cell(6, fill=hea, name='str2', region=STR2)
blanket = openmc.Cell(7, fill=flibe, name='blanket', region=BLANKET)
#shield = openmc.Cell(8, fill=wc, name='shield', region=SHIELD)

root_universe = openmc.Universe(cells=(plasma, first_wall, str1, channel, nmult, str2,
blanket))
geometry = openmc.Geometry(root_universe)
geometry.export_to_xml()

##############################################################################
#Geometry plotting 2D
plotg = openmc.Plot()
plotg.filename = 'D_model'
plotg.basis = 'xz'
plotg.width = (247*2, 247*2)
plotg.pixels = (400, 400)
plotg.origin = (330, 0, 0)
plotg.color_by = 'material'
plotg.colors = {void: 'white', w: 'red', hea: 'lightslategrey', flibe: 'aqua'}
#plotg.colors = {void: 'white', w: 'red', hea: 'lightslategrey', flibe: 'aqua', wc: 'olive'}
plotg.background = 'black'

plots = openmc.Plots([plotg])
plots.export_to_xml()
openmc.plot_geometry()


##############################################################################
```

```
# Define problem settings

# Indicate how many particles to run
settings = openmc.Settings()
batches = 30
settings.batches = batches
settings.inactive = 10
settings.particles = 50000
settings.run_mode = 'fixed source'

# Create an initial source

my_plasma = TokamakSource(
    #elongation=1.557,
    elongation=1.84,
    #ion_density_centre=1.09e20,
    ion_density_centre=1.8e20,
    ion_density_peaking_factor=1,
    ion_density_pedestal=1.05e20,
    ion_density_separatrix=1e20,
    #ion_temperature_centre=45.9,
    ion_temperature_centre=27,
    ion_temperature_peaking_factor=8.06,
    ion_temperature_pedestal=2.5,
    ion_temperature_separatrix=0.5,
    major_radius=330,
    minor_radius=60,
    pedestal_radius=0.8 * 60,
    mode="H",   # 3 MODES: H, L, A.  We use 'H' as suggested in [1]
    #shafranov_factor=0.44789,
    shafranov_factor=0.44789,
    triangularity=0.270,
    ion_temperature_beta=6
    )

settings.source = my_plasma.sources

settings.export_to_xml()

###############################################################################
# Define tallies

# Instantiate an empty Tallies object
tallies = openmc.Tallies()

# Create mesh which will be used for tally
mesh = openmc.RegularMesh()
mesh.dimension = [500, 1, 500]
mesh.lower_left = [80, -250, -250]
mesh.upper_right = [580, 250, 250]
```

```
# Create mesh filter for tally
mesh_filter = openmc.MeshFilter(mesh)

# Create mesh tally to score tritium rate production
cell_filter = openmc.CellFilter([channel.id, nmult.id, blanket.id])
tbr_tally = openmc.Tally(name='TBR')
tbr_tally.filters = [cell_filter]
tbr_tally.scores = ['H3-production']
tallies.append(tbr_tally)

# Create mesh tally to score neutron flux
#cell_filter2 = openmc.CellFilter([fw.id, str1.id, flibe1.id, multiplier.id, str2.id, flibe2.id])
flux_plot_tally = openmc.Tally(name='Flux')
flux_plot_tally.filters = [mesh_filter]
flux_plot_tally.scores = ['flux']
tallies.append(flux_plot_tally)

# Create mesh tally to score tritium rate production in mesh filter to plot Tritium generation
tbrplot_tally = openmc.Tally(name='TBR all values')
tbrplot_tally.filters = [mesh_filter]
tbrplot_tally.scores = ['H3-production']    #usato al posto di (n,t)
tallies.append(tbrplot_tally)

# Create mesh tally to score neutron spectra
energy_bins = openmc.mgxs.GROUP_STRUCTURES['CCFE-709']
energy_filter = openmc.EnergyFilter(energy_bins)
str1_filter = openmc.CellFilter([str1.id])
str2_filter = openmc.CellFilter([str2.id])

spectrastr1_tally = openmc.Tally(name='structural_layer_spectra_STR1')
spectrastr1_tally.filters = [str1_filter, energy_filter]
spectrastr1_tally.scores = ['flux']
tallies.append(spectrastr1_tally)

spectrastr2_tally = openmc.Tally(name='structural_layer_spectra_STR2')
spectrastr2_tally.filters = [str2_filter, energy_filter]
spectrastr2_tally.scores = ['flux']
tallies.append(spectrastr2_tally)

# Export to "tallies.xml"
tallies.export_to_xml()

###############################################################################
# Run OpenMC!
openmc.run()

###############################################################################
```

```
#Tally Data Processing
# Load the statepoint file
sp = openmc.StatePoint('statepoint.30.h5')

tally = sp.get_tally(scores=['flux'])

flux = tally.get_slice(scores=['flux'])
flux.std_dev.shape = (500, 500)
flux.mean.shape = (500, 500)

plt.imshow(flux.mean, interpolation='nearest', cmap='jet')
plt.title('Flux distribution')
plt.xlabel('x [cm]')
plt.ylabel('y [cm]')
plt.colorbar()
plt.show()

tbrplot_tally = sp.get_tally(name='TBR all values')
tbrplot_tally.std_dev.shape = (500, 500)
tbrplot_tally.mean.shape = (500, 500)

plt.imshow(tbrplot_tally.mean, interpolation='nearest', cmap='inferno')
plt.title('Tritium generation mean result')
plt.xlabel('x [cm]')
plt.ylabel('y [cm]')
plt.colorbar()
plt.show()

plt.imshow(tbrplot_tally.std_dev, interpolation='nearest', cmap='inferno')
plt.title('Tritium generation standard deviation')
plt.xlabel('x [cm]')
plt.ylabel('y [cm]')
plt.colorbar()
plt.show()

tbr_tally = sp.get_tally(name='TBR')
tbr_result = tbr_tally.get_pandas_dataframe()
yy = tbr_result['mean']
tbr_total = round(yy.sum(), 3)

zz = tbr_result['std. dev.']
error = round(zz.sum(), 4)
print('************************************************************')
print('************************************************************')
print('TBR PRODUCTION IN FLiBe')
print(tbr_result)
print('************************************************************')
print('************************************************************')
print('TBR total IN FLiBe')
print(tbr_total, '+/-', error)
```

```
#Source plotting 2D and 3D
plot_tokamak_source_3D(my_plasma, "neutron_source_density")
plt.title('Neutron source density 3D')
plt.show()


scatter_tokamak_source(my_plasma, "neutron_source_density")
plt.colorbar(label='Neutron source density [neutrons/s/m3]')
plt.show()

scatter_tokamak_source(my_plasma, "ion_temperature")
plt.colorbar(label='Ion temperature [keV]')
plt.show()

###############################################################################
#Geometry & Source plotting 2D
scatter_tokamak_source(my_plasma, "ion_temperature")
plt.colorbar(label='Ion temperature [keV]')
root_universe.plot(width=(1000, 1000), basis='xz', alpha=0.5,
                   colors={plasma: 'white', first_wall: 'red',
                   str1: 'lightslategrey', channel: 'aqua',
                   nmult: 'aqua', str2: 'lightslategrey',
                   blanket: 'aqua'})
plt.title('Source inside geometry')
plt.show()

# Plot neutron spectra on STR1
spectrastr1_tally = sp.get_tally(name='structural_layer_spectra_STR1') # add another tally
spectrastr1_tally_result = [entry[0][0] for entry in spectrastr1_tally.mean]
spectrastr1_tally_std_dev = [entry[0][0] for entry in spectrastr1_tally.std_dev]

spectrumstr1 = []
spectrumstr1.append(0)
spectrumstr1.extend(spectrastr1_tally_result)

plt.loglog(energy_bins, spectrumstr1, linewidth=1)
plt.xlabel('Energy eV'
plt.ylabel('Neutrons per cm2 per source neutron')
plt.title('Neutron spectra STR1')
plt.grid(True, which="both", ls="--", color='0.65')
plt.show()
```

```
traces=[]
traces.append(Scatter(x=energy_bins,
                      y=spectrastr1_tally_result,
                      name='breeder_blanket_spectra_STR1',
                      line=dict(shape='hv')
                     )
              )

layout = {'title':'Neutron spectra STR1',
          'hovermode':'closest',
          'xaxis':{'title':'Energy eV',
                   'type':'log'},
          'yaxis':{'title':'Neutrons per cm2 per source neutron',
                   'type':'log'},
          }
plot({'data':traces,
      'layout':layout
     },
       filename='STR1_spectra.html'
    )

# Plot neutron spectra on STR2
spectrastr2_tally = sp.get_tally(name='structural_layer_spectra_STR2') # add another tally
spectrastr2_tally_result = [entry[0][0] for entry in spectrastr2_tally.mean]
spectrastr2_tally_std_dev = [entry[0][0] for entry in spectrastr2_tally.std_dev]

spectrumstr2 = []
spectrumstr2.append(0)
spectrumstr2.extend(spectrastr2_tally_result)

plt.loglog(energy_bins, spectrumstr2, linewidth=1)
plt.xlabel('Energy eV')
plt.ylabel('Neutrons per cm per source neutron')
plt.title('Neutron spectra STR2')
plt.grid(True, which="both", ls="--", color='0.65')
plt.show()
```

Appendix B

Example of inventory input file for FISPACT-II for High-entropy alloy in the first layer of the vacuum vessel.

```
CLOBBER
JSON
GETXS 0
GETDECAY 0
FISPACT
* FNS  1 year alloy A
DENSITY 12.36
MASS 1.0E-3 5
V 30.00
CR 10.00
W  40.00
TA 10.00
TI 10.00
MIND 1E3
GRAPH 3 2 1
  3 1 2

UNCERTAINTY 2
HALF
HAZARDS
<< -----irradiation phase----- >>
FLUX 7.54E+14
ATOMS
TIME 1.0 YEARS
ATOMS
```

<< -----cooling phase----- >>

FLUX 0.

ZERO

TIME 1 SECS ATOMS

TIME 4 SECS ATOMS

TIME 25 SECS ATOMS

TIME 30 SECS ATOMS

TIME 1 MINS ATOMS

TIME 3 MINS ATOMS

TIME 5 MINS ATOMS

TIME 20 MINS ATOMS

TIME 30 MINS ATOMS

TIME 1 HOURS ATOMS

TIME 4 HOURS ATOMS

TIME 6 HOURS ATOMS

TIME 12 HOURS ATOMS

TIME 1 DAYS ATOMS

TIME 2 DAYS ATOMS

TIME 3 DAYS ATOMS

TIME 7 DAYS ATOMS

TIME 17 DAYS ATOMS

TIME 31 DAYS ATOMS

TIME 123 DAYS ATOMS

TIME 184 DAYS ATOMS

TIME 1 YEARS ATOMS

TIME 2 YEARS ATOMS

TIME 2 YEARS ATOMS

TIME 2 YEARS ATOMS

TIME 2 YEARS ATOMS

TIME 2 YEARS ATOMS

TIME 2 YEARS ATOMS

TIME 2 YEARS ATOMS

TIME 2 YEARS ATOMS

TIME 2 YEARS ATOMS

TIME 5 YEARS ATOMS
TIME 5 YEARS ATOMS
TIME 5 YEARS ATOMS
TIME 5 YEARS ATOMS
TIME 5 YEARS ATOMS
TIME 5 YEARS ATOMS
TIME 10 YEARS ATOMS
TIME 10 YEARS ATOMS
TIME 10 YEARS ATOMS
TIME 10 YEARS ATOMS
TIME 10 YEARS ATOMS
TIME 25 YEARS ATOMS
TIME 25 YEARS ATOMS
TIME 25 YEARS ATOMS
TIME 25 YEARS ATOMS
TIME 50 YEARS ATOMS
TIME 50 YEARS ATOMS

END
* END
/*

References

[1] Camera dei deputati, Servizio Studi XVIII Legislatura, "Cambiamenti climatici," 2022.

[2] B.N. Sorbom, et al., "ARC: A compact, high-field, fusion nuclear science facility anddemonstration power plant with demountable magnets," *Fusion Engineering and Design,* vol. 100, pp. 378-405, 2015.

[3] S. Segantin, et al., "ARC reactor – Neutron irradiation analysis," *Fusion Engineering and Design,* vol. 159, no. 111792, 2020.

[4] B. Bocci, et al., "ARC reactor materials: Activation analysis and optimization," *Fusion Engineering and Design,* vol. 154, no. 111539, 2020.

[5] J. Kenneth Shultis, Richard E. Faw, Fundamentals of Nuclear Science and Engineering, Taylor & Francis, 2002, p. 520.

[6] Raymond L. Murray, Keith E. Holbert, Nuclear Energy: An Introduction to the Concepts, Systems, and Applications of Nuclear Processes (Seventh Edition), Oxford: Butterworth-Heinemann, 2015.

[7] Jeffrey P. Freidberg, PLASMA PHYSICS AND FUSION ENERGY, Cambridge University Press, 2007.

[8] Mitsuru Kikuchi, Karl Lackner, Minh Quang Tran, FUSION PHYSICS, IAEA International Atomic Energy Agency, 2012.

[9] H. Jiang, et al., "Optimal Tracking for a Divergent-Type Parabolic PDE System in," *Hindawi Publishing Corporation,* vol. 2014, pp. 1-8, 2014.

[10] W. Biel, F. Cismondi, "Tritium Breeding and blanket technology," 26 09 2014. [Online]. Available: https://www.dpg-physik.de/veranstaltungen/2014/biel2.pdf.

[11] Eni, "Eni e CFS: raggiunto un traguardo fondamentale nella ricerca sulla fusione a confinamento magnetico," 08 09 2021. [Online]. Available: https://www.eni.com/it-IT/media/comunicati-stampa/2021/09/cs-eni-cfs-raggiunto-fusione-confinamento-magnetico.html.

[12] J. Bardeen, ET AL., "Microscopic Theory of Superconductivity," *Heating up of Superconductors,* 1957.

[13] Z.S. Hartwig, et al., "An initial study of demountable high-temperature superconducting toroidal field magnets for the Vulcan tokamak conceptual design," *Fusion Engineering and Design,* vol. 87, 2012.

[14] A. Q. Kuang, et al., "Conceptual design study for heat exhaust management in the ARC fusion," *Fusion Engineering and Design,* vol. 137, pp. 221-242, 2018.

[15] M. Kondo, et al., "High Performance Corrosion Resistance of Nickel-Based Alloys in Molten Salt Flibe," *Fusion Science and Technology,* vol. 56, pp. 190-194, 2009.

[16] S. Segantin, et al., "Optimization of tritium breeding ratio in ARC reactor," *Fusion Engineering and Design,* vol. 154, p. 111531, 2020.

[17] Massimiliano Balzano, "Chimichiamo," [Online]. Available: https://www.chimicamo.org/chimica-fisica/leghe-ad-alta-entropia/.

[18] Damian Sobieraj, et al., "Chemical short-range order in derivative Cr–Ta–Ti–V–W high entropy alloys from the first-principles thermodynamic study," *Physical Chemistry Chemical Physics,* 2020.

[19] Massachusetts Institute of Technology, “OpenMC,” [Online]. Available: https://docs.openmc.org/en/stable/index.html.

[20] A. Thomas, et al., “High temperature deformation of Inconel 718,” *Journal of Materials Processing Technology,* vol. 177, pp. 469-472, 2006.

[21] Clement Fausser, et al., “Tokamak D-T neutron source models for different plasma physics confinement modes,” *Fusion Engineering and Design,* vol. 87, pp. 787-792, 2012.

[22] OpenMC, “PyPI The Python Package Index,” [Online]. Available: https://pypi.org/project/openmc-plasma-source/.

[23] O. A. Waseem.et al., “Powder Metallurgy Processing of a WxTaTiVCr High-Entropy Alloy and Its Derivative Alloys for Fusion Material Applications,” *Scientifc Reports,* vol. 7, no. 1926, 2017.

[24] Wikipedia, “Tungsten,” [Online]. Available: https://en.wikipedia.org/wiki/Tungsten.

[25] Michael Fleming, Thomas Stainer, Mark Gilbert, The FISPACT-II User Manual, Abingdon: UNITED KINGDOM ATOMIC ENERGY AUTHORITY, 2018.

[26] IAEA International Atomic Energy Agency, “Classification of Radioactive Waste - General Safety Guide No.GSG-1,” IAEA.

[27] MassimoZucchetti, et al., “Radioactive Waste Management of Fusion Power Plants,” *Radioactive Waste ,* pp. 303-328, 2012.

[28] Toshimasa Yoshiie, et al., “Defect structural evolution in high purity tungsten irradiated with electrons using high voltage electron microscope,” *Journal of Nuclear Materials,* vol. 343, 2005.

[29] Vijay K.Panday, et al., “Determination of trace impurities in tantalum by inductively coupled plasma mass spectrometry after removal of the matrix by liquid-liquid extraction,” *Analytica Chimica Acta,* vol. 329, pp. 153-159, 1996.